

AN APPLICATION-ORIENTED FRAMEWORK FOR CONTINUUM MODELING OF OPINION DYNAMICS ON A NETWORK

GIANLUCA FAVRE , GASPARD JANKOWIAK , SARA MERINO-ACEITUNO ,
AND LARA TRUSSARDI 

ABSTRACT. In this article, we propose a modeling framework to develop a continuum description of opinion dynamics on networks. Our primary objective is to present a continuum approach that is practical for applications, particularly for numerical simulations. While existing methods, such as graphons, offer continuum descriptions in the large-node limit, their abstract mathematical nature limits their applicability to real-world scenarios, such as modeling opinion dynamics. To illustrate our framework, we focus on a simple model of consensus dynamics on a network and derive a continuum description using techniques inspired by mean-field limits. We also discuss the limitations of this approach and suggest extensions to account for dynamic networks with evolving connections, stochastic effects, and directional interactions.

1. INTRODUCTION

The continuum description of graphs is a challenging mathematical problem, particularly the derivation of continuum models from discrete ones. A well-established approach is through graphons [43, 45, 52], typically for dense graphs, and their extensions, such as graphops [51], for sparse graphs. However, graphons and their generalizations are mathematically abstract objects that are difficult to apply in practice or adapt to dynamical networks.

As an alternative, kinetic approaches, like mean-field limits, have been employed to study network dynamics. In [25] for instance, the authors derived continuum equations for networks of fibers, with further developments in [7, 6, 8]. In that model, fibers are characterized by spatial position and orientation. In contrast, opinion dynamics involves a single variable: the opinion. This fundamental difference limits the applicability of the approach in [25] to opinion models, as we will illustrate later.

We focus on Abelson's model [1], a simple opinion consensus model where individuals interact pairwise through their social network. At the discrete level, we consider $N > 1$ individuals, each characterized by an opinion $\omega_i(t) \in \mathbb{R}$ at time $t \in \mathbb{R}_+$ with $i = 1, \dots, N$, connected via a fixed network. Our objective is to develop a continuum framework for these dynamics, suitable for practical applications and numerical simulations.

Specifically, we introduce a continuum description based on two quantities: the opinion density $f = f(\omega)$, and the edge distribution $g = g(\omega, m)$. The density f represents the proportion

of individuals with opinion ω , and is the limiting object obtained through classical mean-field limits. In the discrete setting, $f(\omega)$ can be understood as the number of individuals with opinion ω divided by the total population. The edge distribution g is a new object that does not appear in classical mean-field limits: $g(\omega, m)$ gives the proportion of links between pair of individuals with opinions ω and m . At the discrete level, $g(\omega, m)$ can be understood as the number of connected individuals with opinions m and ω divided by the total number of connections in the network. Since the social network is undirected, g is symmetric: $g(\omega, m) = g(m, \omega)$. In the same way that f does not capture information about individual agents (since it only reflects the average opinion), the edge distribution g represents the probability of two individuals holding different opinions being connected, but it does not encode the full structure of the discrete network.

We propose a system of partial differential equations governing the evolution of f and g by applying mean-field techniques. The primary challenge is that unlike classical systems, network dynamics cannot be fully captured by averaged behavior alone. By adding an extra piece of information, the edge distribution g , we aim to bridge this gap. However, due to the complexity of network dynamics, there are few rigorous results that use mean-field limits. For related rigorous results, see [8, 5]. In this article, we explain how mean-field limits apply in this context and highlight their limitations, particularly the key challenge: distinguishing between individuals.

To illustrate further the difference between mean-field dynamics and network-induced dynamics, consider a classical mean-field set-up where an agent i with opinion ω interacts with all agents j with opinion m if $|\omega - m| < R$ for some $R > 0$. Crucially, determining if i and j interact only requires knowledge of the respective opinions ω and m , not their individual labels. This enables a mean-field description that is label-independent and based on the concept of exchangeability: interchanging labels yields statistically equivalent systems.

In network-based dynamics, the situation is different. Whether individuals with opinions ω and m influence each other depends on the connectivity between them, and such connectivity is described through the individuals' labels. Two individuals with opinions ω and m may be connected, while another pair with the same opinions may not. Thus, in network-mediated systems, the labels and their associated connections are critical, making it impossible to determine if two individuals interact from just knowing their individual opinions.

To perform a mean-field limit for the opinion model, we need a label-independent representation of the network. For this, instead of tracking an individual's label and opinion, (i, ω) , we consider only its opinions ω . If an individual i with opinion ω is connected to an individual j with opinion m , we just say that ω is connected to m , disregarding labels. This approach works in simple cases but fails when multiple individuals share the same opinion ω . We will discuss strategies to address this limitation, which involve augmenting the system with additional information to distinguish between individuals with identical opinions. Each specific system will require a tailored approach to incorporate this information. As an example, we demonstrate

how this can be achieved for the Lancichinetti-Fortunato-Radicchi (LFR) type networks, which mimic community structures.

The continuum system of equations for f and g that we propose is formally derived under several assumptions. To test the accuracy of the continuum model, first, we verify that it preserves key structural properties of the discrete system; second, we compare the discrete and continuum models numerically.

1.1. The opinion model and the associated network. Our goal is to introduce a continuum modeling framework for opinion dynamics on a network. To this end, we consider a simple model for opinion consensus: the Abelson model. The key difference between this model and the Hegselmann-Krause (HK) model [47] lies in the interaction mechanism. In the HK model, agents interact based on the proximity of their opinions, whereas in Abelson's model, interactions occur only between agents connected by a pre-existing, fixed network. We assume that the network is undirected, a feature observed in social networks like BeReal, Snapchat, and earlier versions of Facebook.

For the numerical comparison between the discrete and continuum models, we use LFR-type graphs [54], a well-known benchmark for testing community behavior. The population is divided into a fixed number of communities, where individuals within the same community share similar opinions. We perform simulations by varying the number of connections between communities, ranging from well-mixed to segregated networks.

In general, consensus is eventually reached as long as the network does not have disconnected components. However, the rate of convergence to consensus depends on the network structure and the connectivity between agents. We investigate this property through numerical simulations for both the discrete and continuum models.

1.2. Some background on social models and social networks. The first formal models of the dynamics of opinion formation in a group were inspired by [2, 39, 46]. The basic idea in these works is that if two members of a group interact, "each member of the group changes his attitude position towards the other by some constant fraction of the 'distance' between them" [2]. We note thus that we have a link with the concept of homophily. In the works of [2, 10, 27, 46, 56], it was analytically shown that for a broad class of models with repeated social influence, consensus is always reached unless the network of interactions is disconnected. For a very good overview of models of social influence, we suggest the reading of [37].

In these models, individuals are treated as nodes in a network. Nodes are connected by a network link if they exert influence on each other. The network links are assumed to be fixed, but they could be weighted. The weights represent the strength of social influence that one individual exerts upon another. This could represent, for example, the social status, or the frequency of interaction. Models as [47] of assimilative influence, with continuous opinions and fixed influence weights, are also often called "classical" models in the literature. Such

classical averaging models assume that opinions vary on a continuous scale and implement social influence as averaging [41, 40].

The model we suggest here falls into such a category. The key idea is that individuals which are connected always influence each other towards reducing opinion differences. As a result, if the network is fully connected, the dynamic (with continuous opinions) inevitably generate consensus in the long run.

In 2000, a sociophysic model for opinion dynamics [50] including “social validation” and “discord destroys” effects was studied. Afterward, in [69], such a model was considered on network.

Another important branch of models has been inherited from the study of birds flocking — or more generally from the study of the behavior of groups of animals — introducing bounded confidence models. The work of Deffuant and Weisbuch [24] is one of the most known example: it presents randomness in the choice of the interactions pairs, which are randomly chosen at each time step.

Several properties like convergence to consensus, clustering, dependence of the equilibrium from the initial data have been well investigated and studied (see for example [10, 30, 31, 48, 72]). The role of the network’s structure in the last decade is gaining more and more importance since, nowadays, opinion travels mainly through social media and social networks. Different models for opinion formation, also including a network structure, attracted a lot of interests [15, 34, 35, 53, 59, 61, 62, 70, 14, 11, 67, 17, 45]. Anyhow, the description of opinion on networks covers a wide range of fields, from mathematics [3, 16, 17, 43, 58], to philosophy [22, 66, 74], through computational social science [9].

There is a growing interest in the kinetic theory community to investigate group behavior in social systems, and a correspondingly growing number of contributions[33, 26, 29], but not all of them are based on networks.

While the discrete description of opinion formation on a network is getting more and more attention, the passage to the continuum level is more delicate since the network structure is lost. To the authors’ knowledge, the question of how to move to a mesoscopic and macroscopic level is somehow still open. We mention some works who addressed this question: [32] considered a mean field limit for the Deffuant opinion dynamics; in [5], the authors studied a mean field limit with time varying weight; in [4, 44, 49] the authors investigate heterogeneous (non-exchangeable) mean-field limits.

1.3. Structure of the paper. In Section 2, we describe the discrete model. In Section 2.2 we consider it in the specific case of consensus dynamics and offer a review of mathematical properties of convergence to consensus. In Section 2.2.2, we propose a continuum model to approximate the discrete dynamics when the number of individuals grows large. We start by defining the node and edge distributions in Section 3.1. After the derivation of the continuum

equations in Sections 3.2 and 3.3, we investigate its mathematical properties in the case of consensus dynamics in Section 3.4. In Section 4, we present refinements of the continuous model. In Section 5, we compare numerically discrete and continuum models. Finally, we present extensions of the model in Section 6. Limitations and open problems are discussed in Section 7.

2. DISCRETE DYNAMICS

2.1. General model. We consider a population of $N > 1$ individuals, each having a certain opinion that evolves over time: $\omega_i = \omega_i(t)$, $\omega_i : \mathbb{R}^+ \rightarrow \Omega$, with $i = 1, \dots, N$ and $\Omega \subset \mathbb{R}$ a connected set.

Moreover, we assume that individuals are part of a network, which is modelled as a loopless, unweighted, undirected graph, where each node corresponds to an individual. Such a graph can be described by the *adjacency matrix* $A = (A_{ij}) \in \{0, 1\}^{N \times N}$. We say that two individuals i and j are connected if there is an edge between the corresponding nodes, and we then write $i \sim j$. In terms of the entries A_{ij} , we have $A_{ij} = 0$ if and only if $i \not\sim j$. In particular, we will assume the following.

Assumption 2.1. *The graph A is connected, and $A_{ij} = A_{ji}$ and $A_{ii} = 0$ for all $i, j = 1, \dots, N$. This assumption means that there is no self-interaction.*

The evolution of each opinion $\omega_i = \omega_i(t)$ is given by:

$$(1) \quad \frac{d}{dt} \omega_i(t) = \frac{1}{\#\mathcal{S}_i} \sum_{j \in \mathcal{S}_i} \mathbf{D}(\omega_i(t) - \omega_j(t)),$$

The function $\mathbf{D} : \mathbb{R} \rightarrow \mathbb{R}$ is the so-called *debate operator* and models pair-wise interactions. The set \mathcal{S}_i , defined as $\mathcal{S}_i = \{j : A_{ij} = 1\}$, represents the individuals j connected with the individual i through the network; and $\#\mathcal{S}_i$ denotes the cardinality of this set. The presence of the weight $(\#\mathcal{S}_i)^{-1}$ appears also in other models for collective dynamics and opinion formation [59, 26] and it models that when two individuals interact, the one with more connections gets less influenced than the other (see e.g. [63]). We also note that the model can be extended to $\Omega \subset \mathbb{R}^d$, for $d \geq 1$, but here we will consider only the one-dimensional case.

2.2. Case of consensus dynamics. To compare the discrete model (1) and the continuum model proposed in this article (Section 2.2.2), we will focus on the particular case of consensus dynamics, for which the system reaches equilibrium asymptotically in time. We will compare both models in terms of their asymptotic behavior.

We assume that $\Omega = (-1, 1)$ and that during pair-interactions individuals' opinions relax towards a common opinion (consensus). To capture this consensus dynamics, we make the following assumption:

Assumption 2.2. *It holds that $\mathbf{D}(z) = -\partial_z W(z)$ for all $z \in \mathbb{R}$, where $W \geq 0$ is a smooth strictly convex potential with a unique global minimum at $z = 0$. Moreover, we choose W even, i.e., $W(z) = W(|z|)$.*

Note that this implies that \mathbf{D} is decreasing, with $\mathbf{D}(0) = 0$. The simplest example is the quadratic potential $W(z) = z^2/2$, and in this case $\mathbf{D}(\omega_i - \omega_j) = \omega_j - \omega_i$.

Through the whole paper, we are going to work under Assumptions 2.1 and 2.2. These are enough to ensure global existence and uniqueness of the solutions.

2.2.1. Convergence to equilibrium. In this Section, we review some mathematical properties of (1). In particular, we focus on the convergence to consensus. At the particle level, the following holds:

Lemma 2.3 (Conserved quantity). *For all times, it holds that*

$$(2) \quad \sum_{i=1}^N \# \mathcal{I}_i \omega_i(t) = \sum_{i=1}^N \# \mathcal{I}_i \omega_i(0).$$

Proof. We compute the time derivative of the left-hand-side of (2), which gives

$$\sum_{i=1}^N \# \mathcal{I}_i \left(\frac{1}{\# \mathcal{I}_i} \sum_{j \in \mathcal{I}_i} \mathbf{D}(\omega_i - \omega_j) \right) = \sum_{i=1}^N \sum_{j \in \mathcal{I}_i} \mathbf{D}(\omega_i - \omega_j) = 0,$$

We recall now that \mathbf{D} is odd, i.e. $\mathbf{D}(\omega_j - \omega_i) = -\mathbf{D}(\omega_i - \omega_j)$. Additionally, we observe that if an individual i is connected with an individual j , i.e. $j \in \mathcal{I}_i$, then it also holds $i \in \mathcal{I}_j$. These two properties implies that all the terms in the sum cancel out, and the sum is thus equal to zero. \square

The proposition above shows that the total weighted opinion of the network (2) is a conserved quantity. We emphasize that Assumption 2.2 is fundamental for this conservation property to hold.

Proposition 2.4 (Convergence to consensus). *Suppose that the graph is connected (Assumption 2.1), then it follows that*

$$\omega_i(t) \rightarrow \omega_\infty^{micro} \text{ as } t \rightarrow \infty, \forall i,$$

where ω_∞^{micro} is the weighted averaged opinion

$$(3) \quad \omega_\infty^{micro} := \frac{1}{\sum_{j=1}^N \# \mathcal{I}_j} \sum_{i=1}^N \# \mathcal{I}_i \omega_i(t=0).$$

Remark 2.5. We observe that the connectedness Assumption 2.1 is essential, without it one would expect different limiting values in general, one for each of the connected components.

The proof of Proposition 2.4 is based on a Lyapunov functional.

Proof of Prop. 2.4. Define the global potential

$$(4) \quad V(\omega_1, \dots, \omega_N) := \frac{1}{2} \sum_{i=1}^N \sum_{j \in \mathcal{J}_i} W(\omega_i - \omega_j).$$

Due to the Assumption 2.2, it holds that

$$\begin{aligned} \frac{d\omega_i(t)}{dt} &= \frac{1}{\#\mathcal{J}_i} \sum_{j \in \mathcal{J}_i} \mathbf{D}(\omega_i - \omega_j) \\ &= -\frac{1}{\#\mathcal{J}_i} \sum_{j \in \mathcal{J}_i} \partial_{\omega_i} W(\omega_i - \omega_j) \\ &= -\frac{1}{\#\mathcal{J}_i} \partial_{\omega_i} V, \end{aligned}$$

where we used that W is even to compute $\partial_{\omega_i} V$.

Thus

$$\begin{aligned} \frac{d}{dt} V(\omega_1(t), \dots, \omega_N(t)) &= \sum_{i=1}^N \partial_{\omega_i} V \frac{d\omega_i}{dt} \\ &= -\sum_{i=1}^N \frac{1}{\#\mathcal{J}_i} (\partial_{\omega_i} V)^2 \\ &\leq -\min\{(\#\mathcal{J}_1)^{-1}, \dots, (\#\mathcal{J}_N)^{-1}\} |\nabla V|^2 \\ (5) \quad &\leq 0. \end{aligned}$$

Since V is the sum of strictly convex functions, it is strictly convex and in this case it has a unique critical point corresponding to the minimum. Indeed, the minimum of V is attained when

$$W(\omega_i - \omega_j) = 0 \quad \text{for all } i \sim j,$$

which holds if and only if $\omega_i = \omega_j$ for all $i \sim j$, by Assumption 2.2. Since we assume that the graph has only one connected component, this implies that all constant solutions, i.e., $\omega_i = \omega_\infty^{\text{micro}}$ for all i for some $\omega_\infty^{\text{micro}}$ are minimizers of V . At the same time, thanks to having a conserved quantity (Lemma 2.3), we know that it must hold that

$$\sum_{i=1}^N \#\mathcal{J}_i \omega_i(0) = \sum_{i=1}^N \#\mathcal{J}_i \omega_\infty^{\text{micro}},$$

which determines the value of $\omega_\infty^{\text{micro}}$ given in (3). This means that V is a global Lyapunov function under the dynamics (thanks to (5)) for $\omega_i = \omega_\infty^{\text{micro}}$. We can apply La Salle's principle [55] and conclude that this $(\omega_\infty^{\text{micro}})_{i=1}^N$ is a global attractor. \square

2.2.2. Speed of convergence in the linear case. We will use the simplest scenario corresponding to $\mathbf{D}(z) = z$ to carry out the numerical simulations in Section 5. In this case, it turns out that ω converges to $\omega_\infty^{\text{micro}}$ *exponentially fast*. More precisely we have the following

Proposition 2.6. *If $\mathbf{D}(z) = -z$, there exist positive constants C and α such that*

$$(6) \quad \|\omega_i(t) - \omega_\infty^{micro}\| \leq C \exp(-\alpha t) \|\omega_i(0) - \omega_\infty^{micro}\|.$$

In the present case, this is a standard result of the theory of linear systems, a proof is sketched in Appendix A. This result also holds in more general cases (e.g. time-dependent graphs), see the review of Proskurnikov and Tempo and the references therein[65].

3. CONTINUUM MODELING FRAMEWORK: THE BASICS

When the number of agents is very large (like in many social networks), we are interested in understanding the evolution of the opinions at the level of the population rather than tracking the changes of each individual opinion. For this purpose, a continuum description is more appropriate than a discrete one.

Our goal here is to establish a description for the dynamics of the population that is as simple as possible so that concrete computations and comparison with the discrete dynamics can be carried out. Moreover, this description should be amenable to adding changes to the network so that it can capture dynamical networks, as well as adding noise, and other types of forces (see Section 6). The approach presented here is based on introducing a density distribution of edges, and it is adapted from Degond et al. [25] The overall picture of this framework can be found in Fig. 1.

3.1. Network description: node distribution and edge distribution. The goal of this Section is to find a continuum model that approximates the dynamics of (1) in the limit of a large number of individuals $N \rightarrow \infty$. In particular, we would like to determine the time-evolution for $f = f(t, \omega)$, the distribution of agents with opinion ω at time t .

Large-particle limits are the central theme of mean-field limits. However, model (1), rather than having a mean-field force, it has a network-mediated force (to have a mean-field force the equation should have the sum over all the individuals and not just over the individuals to which one is connected). As a consequence, we cannot apply directly the methodology of mean-field limits. The main bottleneck to apply this methodology is that the network is characterized using the labels of the agents, but one would need that the interactions between the agents can be described with independence of labels. For this reason, we give next a characterization of the network using the opinions of the agents instead of their labels. In this sense, every agent i will be characterized only by its opinion ω_i instead of by its opinion *and* its label.

Specifically, instead of having a node (individual) i with value ω_i , we consider a node ω_i ; and instead of having an edge $\{i, j\}$, we consider an edge $\{\omega_i, \omega_j\}$. The function

$$(7) \quad \phi : (i \mapsto \omega_i(t))_{i=1}^N \quad \text{is a bijection for } t \in [0, T]$$

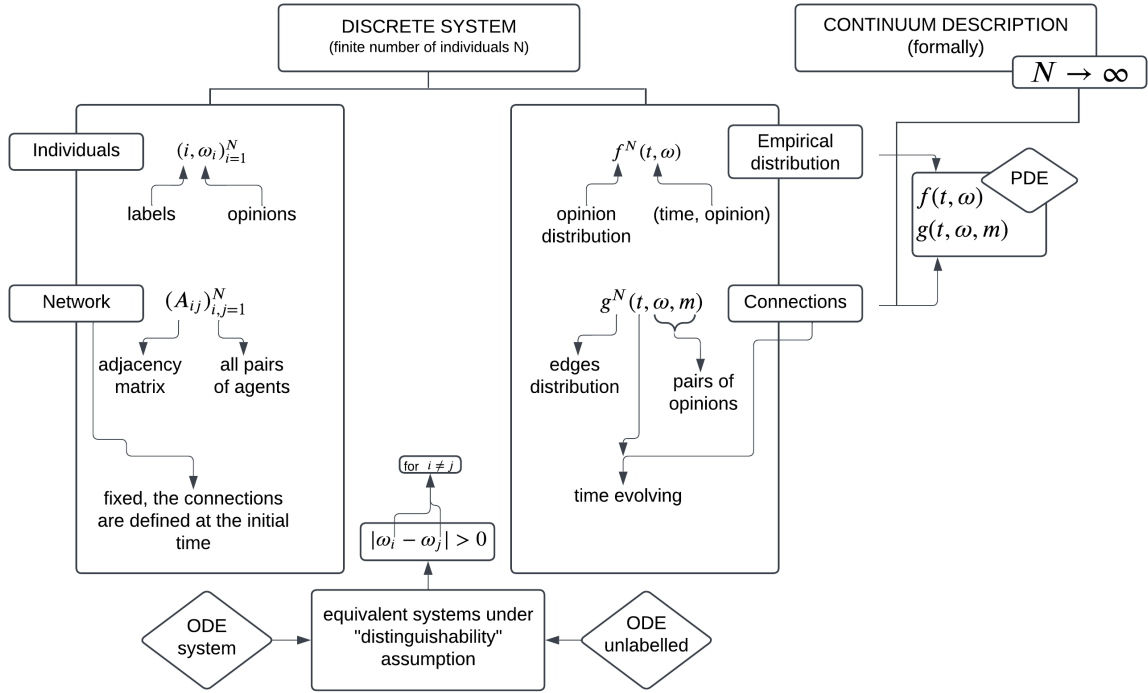


FIGURE 1. **Diagram of the modeling framework.** The discrete system (left) is presented from two perspectives: one describes the evolution of individual opinions $(\omega_i)_{i=1}^N$ over time, where interactions occur on a network represented by the adjacency matrix $(A_{i,j})_{i,j=1}^N$ (see Sec. 2). The other perspective considers the distributions of opinions, f^N , and edges, g^N , as described in Sec. 3.1. Both perspectives yield equivalent sets of ODEs for short times, provided the "distinguishability" assumption 3.1 holds (corresponding to Lemma 3.4). From f^N and g^N , the continuum model is formally derived by taking the limit as $N \rightarrow \infty$ (Sec. 3.3).

between $\{1, \dots, N\}$ and $\{\omega_1(t), \dots, \omega_N(t)\}_{t \in [0, T]}$, as long as $|\omega_i(t) - \omega_j(t)| > r > 0$ for $i \neq j$ and $t \in [0, T]$ and for some r . Thanks to this, we are able to characterize uniquely all the individuals (labels) by just keeping track of the opinions.

For this reason, we make the following assumption:

Assumption 3.1 (Distinguishability assumption). *At $t = 0$, for all $i, j \in \{1, \dots, N\}$, $i \neq j$ it holds for some $r > 0$ that*

$$|\omega_i(0) - \omega_j(0)| > 2r > 0.$$

This assumption extends at least for short times, as explained in the following Lemma:

Lemma 3.2. *Suppose that Assumption 3.1 holds, then for some $T > 0$, and for all times $t \in [0, T]$ and all $i, j \in \{1, \dots, N\}$, $i \neq j$ it holds that*

$$|\omega_i(t) - \omega_j(t)| > r.$$

In particular, (7) holds and, $0 < r = r(N)$ is such that

$$(8) \quad r \leq \inf_{t \in [0, T]} \min_{i \neq j} |\omega_i(t) - \omega_j(t)|.$$

This Lemma is a direct consequence of the continuity of solutions over time.

Since we want to have a continuum description for the interactions in the network, we need to obtain a description for the distribution of the nodes and the distribution of the edges. First, we define the node distribution as the empirical distribution of opinions given by

$$f^N(t, \omega) := \frac{1}{N} \sum_{i=1}^N \delta_{\omega_i(t)}(\omega),$$

where δ_{ω_i} denotes the Dirac delta distribution centered at ω_i . Our goal is to determine the time-evolution for f^N as $N \rightarrow \infty$. Denote by $B_{r/2}(\omega)$ the open ball of radius $r/2$ centered at ω and consider the integral:

$$I(t, \omega_0) := \int_{B_{r/2}(\omega_0)} df^N(t, \omega), \quad \omega_0 \in \Omega, \quad t \in [0, T].$$

Under the notations and the assumptions of Lemma 3.2 we have that $I(t, \omega_0) = 1/N$ if at time t there is an agent with opinion ω_0 and 0 otherwise (by Lemma 3.2 we know that if there is an agent with opinion ω_0 , then this agent is unique, and it is at distance at least r from other opinions). Therefore, in this setup, f^N is able to distinguish between individuals. For this reason, we say that f^N not only captures the distribution of the opinions, but also the nodes of the network.

To have a full description of the network, we need one more ingredient: since we describe the network through the opinions, we also need an evolution for the *description* of the network. The *network* itself is fixed, but the opinions are not, since the opinions evolve over time, the description of the network also evolves over time. This is the price that we have to pay for getting rid of the labels in (1). With this end in mind, we introduce the distribution of edges g^N given by

$$(9) \quad g^N(t, \omega, m) := \frac{1}{2\kappa} \sum_{i \sim j} \delta_{\omega_i(t)}(\omega) \delta_{\omega_j(t)}(m),$$

where κ is the total number of connections (or edges) at initial time (but since the network is fixed, it remains constant). We divide by 2 because in the sum we are counting the pairs twice. Notice that g^N is symmetric in its variables.

Proceeding analogously as before, for $t \in [0, T]$ and $(\omega_0, m_0) \in \Omega^2$ we have that the integral

$$\Gamma(t, \omega_0, m_0) := \int_{B_{r/2}(\omega_0)} \int_{B_{r/2}(m_0)} dg^N(t, \omega, m)$$

satisfies $\Gamma(t, \omega_0, m_0) = \kappa^{-1}$ if at time t there exist two individuals with opinions ω_0 and m_0 (and if this pair exists, it is unique) that are connected via the network; and $\Gamma(t, \omega_0, m_0) = 0$ otherwise. Therefore, from g^N we are able to recover the network.

Moreover, the integral

$$\int_{B_{r/2}(\omega_0)} \int_{\Omega} dg^N(t, \omega, m)$$

is 0 if there is no individual with opinion ω_0 and, if it is different from 0, then it means that there is exactly one individual with that opinion. In this case, the integral corresponds to the total number of connections of ω_0 divided by 2κ . Thus, from this information, one can also recover the information on the nodes, and hence, reconstruct the node density f^N , but, in general, we will have that

$$(10) \quad \int g^N(t, \omega, dm) \neq c f^N(t, \omega), \quad \text{for any constant } c > 0,$$

(the equality is an exception case, and it happens when every individual is connected with all the others. In this case $c = N/(2\kappa)$).

A simple example (illustrated in Figure 2) of this consists of a system with 3 individuals with opinions $\omega_1, \omega_2, \omega_3$, with ω_1 and ω_2 connected and ω_2 and ω_3 connected, so $\kappa = 2$, then

$$f^N(\omega) = \frac{1}{3} (\delta_{\omega_1}(\omega) + \delta_{\omega_2}(\omega) + \delta_{\omega_3}(\omega))$$

and

$$g^N(\omega, m) = \frac{1}{4} \left(\delta_{\omega_1}(\omega) \delta_{\omega_2}(m) + \delta_{\omega_2}(\omega) \delta_{\omega_1}(m) \right. \\ \left. + \delta_{\omega_2}(\omega) \delta_{\omega_3}(m) + \delta_{\omega_3}(\omega) \delta_{\omega_2}(m) \right).$$

We have that

$$\int g^N(\omega, dm) = \frac{1}{4} (\delta_{\omega_1}(\omega) + 2\delta_{\omega_2}(\omega) + \delta_{\omega_3}(\omega)),$$

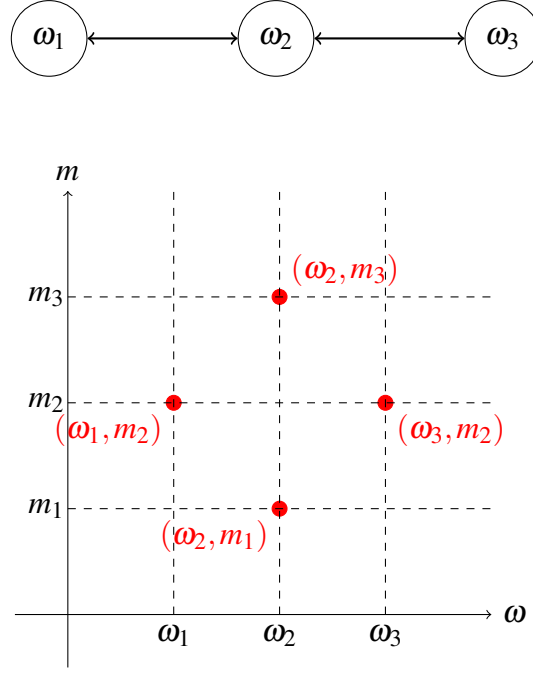
and this does not correspond to a distribution proportional to f^N .

Remark 3.3 (Example: describing the network through the opinions instead of the labels). When we write ω_i , the subscript i indicates that this opinion belongs to individual i . But this notation is a shorthand for the pair (i, ω) , where i represents the individual's label, and ω is their opinion. While with the notation ω_i we compress both pieces of information, it is important to recognize that the label i and the opinion ω are distinct.

Consider a simple network of three agents with the structure given in the diagram in Fig. 2. In this case, the network is described by the edges $1 \leftrightarrow 2$ and $2 \leftrightarrow 3$. Suppose the opinions of these individuals are $(1, 0.5)$, $(2, 0.75)$, and $(3, 0.25)$, where the first entry is the label and the second is the opinion. Since all opinions are distinct, we can alternatively describe the network using the opinions themselves: instead of saying that the network has edges $1 \leftrightarrow 2$ and $2 \leftrightarrow 3$ (in the label space), we can equivalently state that the network has edges $0.5 \leftrightarrow 0.75$ and $0.75 \leftrightarrow 0.25$ (in the opinion space).

This example also highlights the importance of distinguishable opinions: if two individuals have the same opinion, we can no longer differentiate between them or accurately describe the network.

3.1.1. Smoothing of the edge distribution. In this Section, all the integrals are integrals on the domain Ω .

FIGURE 2. Diagram of the network (top) and of its distribution g^N (down)

In the sequel, we will need to evaluate the distribution g^N at some specific opinion ω , which is not possible since we have delta-distributions. For this reason, we introduce a smooth approximation g_r^N of g^N :

$$\begin{aligned}
 g_r^N(\omega, m) &:= \frac{r^2}{2\kappa} \sum_{i \sim j} \delta_{\omega_i(t)}^{(r)}(\omega) \delta_{\omega_j(t)}^{(r)}(m) \\
 (11) \qquad &= \frac{r^2}{2\kappa} \sum_{i=1}^N \sum_{j \in \mathcal{I}_i} \delta_{\omega_i(t)}^{(r)}(\omega) \delta_{\omega_j(t)}^{(r)}(m),
 \end{aligned}$$

where $\delta_{\omega_0}^{(r)}$ is a mollifier, which is a smooth approximation to the δ -distribution centered at $\omega_0 \in \Omega$, i.e., $\delta_{\omega_0}^{(r)} \rightarrow \delta_{\omega_0}$ as $r \rightarrow 0$ in distribution. In particular, we will assume that

$$\begin{aligned}
 &\delta_{\omega_0}^{(r)}(\omega) \text{ compactly supported in } [\omega_0 - r/2, \omega_0 + r/2] \\
 (12) \qquad &\int \delta_{\omega_0}^{(r)} = 1, \text{ and } \delta_{\omega_0}^{(r)}(\omega_0) = \frac{1}{r}.
 \end{aligned}$$

Notice that $r^{-2}g_r^N$ is a probability distribution on $\Omega \times \Omega$ and that

$$\frac{1}{r^2} g_r^N(\omega, m) \rightarrow g^N(\omega, m) \quad \text{as } r \rightarrow 0$$

in distribution.

3.2. An individual-based model with an unlabeled network. We can rewrite our original ODE system (1) as follows:

Lemma 3.4. *Under the assumptions of Lemma 3.2, for $t < T$, the system of equations (1) is equivalent to*

$$(13) \quad \frac{d\omega_i(t)}{dt} = a[g_r^N](\omega_i(t)) + B_r^{(N)}(\omega_i(t)),$$

where $B_r^{(N)} \rightarrow 0$ as $r \rightarrow 0$ for fixed N ($B_r^{(N)}$ is given in (17)), and we defined the operators

$$(14) \quad \begin{aligned} a[g](\omega) &:= \int \eta[g](\omega, m) \mathbf{D}(\omega - m) dm, \\ \eta[g](\omega, m) &:= \frac{g(\omega, m)}{\int g(\omega, m') dm'}, \end{aligned}$$

with $\eta[g](\omega, \cdot) = 0$ if $g(\omega, \cdot) = 0$ a.e..

Proof of Lemma 3.4. Thanks to introducing the approximation of the δ -distributions, we can evaluate g_r^N at a given point $\omega_i(t)$ using (12):

$$\begin{aligned} g_r^N(\omega_i(t), m) &= \frac{r^2}{2\kappa} \sum_{j \in \mathcal{J}_i} \delta_{\omega_i(t)}^{(r)}(\omega_i(t)) \delta_{\omega_j(t)}^{(r)}(m) \\ &= \frac{r}{2\kappa} \sum_{j \in \mathcal{J}_i} \delta_{\omega_j(t)}^{(r)}(m). \end{aligned}$$

Integrating with respect to m and using the fact that the $\delta_{\omega_j(t)}^{(r)}$ have disjoint support (Lemma 3.2), we obtain

$$(15) \quad \int g_r^N(\omega_i, m) dm = \frac{r}{2\kappa} \sum_{j \in \mathcal{J}_i} \int \delta_{\omega_j(t)}(m) dm,$$

and since all integrals in the sum equal one, we have

$$(16) \quad \#\mathcal{J}_i := \frac{2\kappa}{r} \int g_r^N(\omega_i(t), m) dm.$$

We can then rewrite (1):

$$\begin{aligned} \frac{d\omega_i}{dt} &= \frac{1}{\#\mathcal{J}_i} \sum_{j \in \mathcal{J}_i} \mathbf{D}(\omega_i - \omega_j) \\ &= \frac{1}{\#\mathcal{J}_i} \sum_{j \in \mathcal{J}_i} \int \mathbf{D}(\omega_i - m) \delta_{\omega_j}(m) dm \\ &= \frac{1}{\#\mathcal{J}_i} \sum_{j \in \mathcal{J}_i} \int \mathbf{D}(\omega_i - m) \left(\delta_{\omega_j}(m) - \delta_{\omega_j}^{(r)}(m) \right) dm \\ &\quad + \frac{1}{\#\mathcal{J}_i} \sum_{j \in \mathcal{J}_i} \int \mathbf{D}(\omega_i - m) \delta_{\omega_j}^{(r)}(m) dm \\ &=: B_r^{(N)} + C_r^{(N)}, \end{aligned}$$

with

$$\begin{aligned}
B_r^{(N)} &:= \frac{1}{\#\mathcal{J}_i} \sum_{j \in \mathcal{J}_i} \int \mathbf{D}(\omega_i - m) \left(\delta_{\omega_j}(m) - \delta_{\omega_j}^{(r)}(m) \right) dm \\
&= \frac{r}{2\kappa \int g_r^N(\omega_i(t), m) dm} \\
(17) \quad &\times \sum_{j \in \mathcal{J}_i} \int \mathbf{D}(\omega_i - m) \left(\delta_{\omega_j}(m) - \delta_{\omega_j}^{(r)}(m) \right) dm \\
&\rightarrow 0 \text{ as } r \rightarrow 0.
\end{aligned}$$

Using (15) and (16) we also have

$$\begin{aligned}
C_r^{(N)} &:= \frac{1}{\#\mathcal{J}_i} \sum_{j \in \mathcal{J}_i} \int \mathbf{D}(\omega_i - m) \delta_{\omega_j}^{(r)}(m) dm \\
&= \frac{1}{\#\mathcal{J}_i} \frac{2\kappa}{r} \int \mathbf{D}(\omega_i - m) g_r^N(\omega_i, m) dm \\
&= \int \mathbf{D}(\omega_i - m) \frac{g_r^N(\omega_i, m)}{\int g_r^N(\omega_i, m') dm'} dm \\
&= \int \mathbf{D}(\omega_i - m) \eta[g_r^N](\omega, m) dm.
\end{aligned}$$

For $t < T$, it thus holds that

$$(18) \quad \frac{d\omega_i}{dt} = B_r^{(N)} + \int \eta[g_r^N](\omega, m) \mathbf{D}(\omega_i - m) dm,$$

which yields the result. \square

3.3. Large-particle limit $N \rightarrow \infty$. Our goal is to compute formally the limit $N \rightarrow \infty$ for the unlabeled model (13).

Remark 3.5 (Equivalence of the systems). To have that the dynamics of (1) and (13) match, we must consider $r = r(N)$ as given in Lemma 3.2. Then we know that the dynamics for both systems coincide for $t < T$, $T = T(r, N)$. However, forcibly, it must hold that $r(N) \rightarrow 0$ as $N \rightarrow \infty$. Therefore, in the limit, we cannot assume that Lemma 3.4 holds. However, for a fixed given r , the system of ODEs (13) is well-defined and we can take the limit $N \rightarrow \infty$.

Assumption 3.6. Let f^N and g_r^N be defined as above. Suppose that both functions have limits as $N \rightarrow \infty$ (and $r(N) \rightarrow 0$), denoted by f and g — suppose that the convergence is strong enough, and the limiting functions are regular enough (so that we can take the limit and do integration by parts in (23) and in (24) below). Under these assumptions, we take $r(N)$ small enough so that

$$(19) \quad \sum_{i=1}^N |B_{r(N)}^{(N)}| \rightarrow 0 \quad \text{as } N \rightarrow \infty.$$

(This is possible by choosing an approximation of the δ -distribution δ_r that converges to δ fast enough.)

Remark 3.7. Proving rigorously the limit of f^N is a central objective in the study of mean-field limits. Various techniques have been developed for this purpose, such as coupling approaches (see [71, 18]). For a comprehensive treatment, we refer the reader to the monographs [19, 20].

In contrast, establishing the limit of g_r^N is significantly more challenging and it is sometimes assumed [64]. This is the primary difficulty on making this methodology rigorous. It is reasonable to conjecture that the limit of g_r^N requires certain scaling assumptions related to the network size N .

Since the computations that follow are formal, we will assume that limits can be exchanged with derivatives and integrals. In this context, when we require the convergence to be "sufficiently strong", we mean that we assume that the convergence of the functions is such that the formal manipulations performed in the subsequent calculations are justified.

Proposition 3.8 (Large-particle limit for (13)). *Consider f^N and g_r^N under Assumption 3.6. We denote by $f = f(t, \omega)$ and $g = g(t, \omega, m)$ their respective limits. Then, these functions satisfy the following system of equations:*

$$(20a) \quad \partial_t f(\omega) + \partial_\omega (a[g](\omega)f(\omega)) = 0, \quad \omega \in \Omega,$$

$$(20b) \quad \begin{aligned} & \partial_t g(\omega, m) + \partial_\omega (a[g](\omega)g(\omega, m)) \\ & + \partial_m (a[g](m)g(\omega, m)) = 0, \quad (\omega, m) \in \Omega^2, \end{aligned}$$

where $a[g]$ is given in Lemma 3.4.

The initial conditions $f(t=0)$ and $g(t=0)$ are given as the limits of $f^N(t=0)$ and $g^N(t=0)$, respectively.

To ensure the preservation of the total mass, we impose zero flux boundary conditions at the boundary of the domain $\partial\Omega$:

$$(21a) \quad a[g](\omega)f(\omega) = 0, \quad \omega \in \partial\Omega$$

$$(21b) \quad a[g](\omega)g(\omega, m) = 0, \quad (\omega, m) \in \partial\Omega^2.$$

The proof can be found at the end of this Section — we comment first on this result. Equation (20a) gives the evolution for the distribution of opinions $f = f(t, \omega)$. Notice that the equation is in a conservative form, which guarantees that the total mass of individuals is preserved. It can be interpreted as a continuity equation with “velocity” $a[g](\omega)$, i.e., the “velocity” of opinions is dictated by $a[g]$, which describes interactions through the network. The function $\eta(\omega, \cdot)$ in (14) is a probability distribution that gives the distribution of opinions connected to opinion ω . Notice that g is symmetric but η is not.

Since the network is represented via the opinions and the opinions evolve over time, the distribution $g = g(\omega, m)$ also evolves over time. Hence, we get equation (20b) which is again an equation in conservative form (which guarantees that the total density of links is constant over time). It has two terms, one for each one of the variables ω and m . These terms are symmetric

so g is also symmetric, i.e., $g(\omega, m) = g(m, \omega)$. We observe that the equation for g is closed (i.e., it is independent of f). Moreover, if we define the connectivity of an opinion ω as

$$(22) \quad h(\omega) := \int g(\omega, m) \, dm,$$

we observe that h and f satisfy the same equation (one obtains the equation for h by integrating the equation of g against m). However, h and f do not have the same initial data, so they are not the same. In particular, this means that from g we cannot recover f (recall (10) at the discrete level).

Further, notice that in the mean-field limit as it is carried out here, we lose the information of the relation between κ (the total number of connections) and N . Moreover, because of the 0-homogeneity of η in g (i.e. $\eta[\lambda g] = \eta[g]$ for any scalar $\lambda \neq 0$), it holds the following:

Proposition 3.9 (Scaling invariance). *If (f, g) is a solution of system (21) with initial data (f_0, g_0) , then, $(\lambda f, \mu g)$ is a solution with initial data $(\lambda f_0, \mu g_0)$, for any $\lambda, \mu > 0$.*

Even though we do not exploit this property in the current paper, it is a relevant feature of the differential equation that can be used in future mathematical analyses.

The proof is a direct check. In particular, by taking $\lambda = 1$ as required by f being a probability distribution, this means that multiplying the initial datum $g(t = 0)$ by a constant will leave f unchanged. In other words, the density f remains invariant under scaling of the initial data $g(t = 0)$. However, in our case we fix the total integral of $g(t = 0)$ to be 1 to have a probability density.

Prop. 3.8. Let us consider a smooth test function φ compactly supported in the interior of Ω and compute the time derivative of

$$\begin{aligned} \frac{d}{dt} \left(\int \varphi \, df^N \right) &= \frac{d}{dt} \left(\frac{1}{N} \sum_{i=1}^N \varphi(\omega_i(t)) \right) \\ &= \frac{1}{N} \sum_{i=1}^N \varphi'(\omega_i(t)) \frac{d\omega_i}{dt} \\ &= \frac{1}{N} \sum_{i=1}^N \varphi'(\omega_i(t)) a[g_r^N](\omega_i(t)) \\ &\quad + \frac{1}{N} \sum_{i=1}^N \varphi'(\omega_i(t)) B_r^{(N)}(\omega_i(t)) \\ &= \int \varphi'(\omega) a[g_r^N](\omega) \, df^N(t, \omega) \\ &\quad + \frac{1}{N} \sum_{i=1}^N \varphi'(\omega_i(t)) B_r^{(N)}(\omega_i(t)). \end{aligned} \tag{23}$$

Letting $N \rightarrow \infty$, using (19) and integrating by parts, since we assume that f and g are regular enough, we obtain

$$\begin{aligned} \frac{d}{dt} \left(\int \varphi \, df \right) &= \int \varphi'(\omega) a[g](\omega) f(\omega) \, d\omega \\ &= \int \varphi(\omega) \partial_\omega [a[g](\omega)] f(\omega) \, d\omega, \end{aligned}$$

which corresponds to the equation of f (20a) in weak form.

We need a second equation which describes the evolution of g . Let $\varphi = \varphi(\omega, m)$, $\varphi \in C_c^\infty(\Omega \times \Omega)$ be a test function with compact support in the interior of the domain and consider

$$(24) \quad \int \varphi(\omega, m) \, dg_r^N(\omega, m) = \frac{r^2}{2\kappa} \sum_{i \sim j} \varphi(\omega_i, \omega_j).$$

Now, computing the time derivative and integrating by parts, we obtain (proceeding as before) the equation (20b) for g . \square

3.4. Case of consensus dynamics: properties captured from the discrete system. In this Section, we perform an analysis parallel to the one done for the discrete model (Section 2.2) with the aim of checking if the essential structure of the discrete dynamics (1) is captured by the continuum model (20a)–(20b) when we have consensus dynamics (Assumption 2.2).

First, we have the analogous conserved quantity of Lemma 2.3:

Lemma 3.10. *It holds that*

$$(25) \quad \int \int \omega g(t, \omega, m) \, d\omega \, dm = \int \int \omega g(0, \omega, m) \, d\omega \, dm.$$

The proof is a direct check (by time-differentiating). Notice that, indeed, expression (25) is the analogue to the one in the discrete system given in (2).

Second, we can define the analogue of the discrete potential V (4) for the continuum dynamics as:

$$\tilde{V}(t) = \iint W(\omega - m) g(t, \omega, m) \, d\omega \, dm.$$

Third, we obtain a similar ‘‘Lyapunov condition’’ (5) as in the discrete setting for the continuum potential \tilde{V} :

Lemma 3.11. *It holds that*

$$(26) \quad \frac{d}{dt} \tilde{V}(t) \leq -2 \int h(\omega) a^2[g](\omega) \, d\omega \leq 0$$

where h is defined in (22).

Proof. We compute the time derivative of \tilde{V} :

$$\begin{aligned}
& \frac{d}{dt} \left(\int \int W(\omega - m) g(t, \omega, m) d\omega dm \right) \\
&= - \int \int W(\omega - m) \partial_\omega (a[g](\omega) g(\omega, m)) d\omega dm \\
&\quad - \int \int W(\omega - m) \partial_m (a[g](m) g(\omega, m)) d\omega dm \\
&= - 2 \int \int W(\omega - m) \partial_\omega (a[g](\omega) g(\omega, m)) d\omega dm \\
&= - 2 \int \int \mathbf{D}(\omega - m) a[g](\omega) g(\omega, m) d\omega dm \\
&= - 2 \int h(\omega) a^2[g](\omega) d\omega,
\end{aligned}$$

where in the second equality we used that $W(\omega - m) = W(m - \omega)$ and $g(\omega, m) = g(m, \omega)$; and in the third one we used integration by parts, the zero-flux boundary condition (21b), and that $\mathbf{D}(\omega - m) = -\partial_\omega W(\omega - m)$. The last inequality is obtained by multiplying and dividing the integrand by $h(\omega)$ and using that $\eta(\omega, m) = g(\omega, m)/h(\omega)$ and the definitions. \square

In analogy with the discrete system, we will suppose that

$$\begin{aligned}
(27) \quad & f(t, \omega) \rightarrow \delta_{\omega_\infty^{\text{cont}}}(\omega) \\
& g(t, \omega, m) \rightarrow \delta_{\omega_\infty^{\text{cont}}}(\omega) \delta_{\omega_\infty^{\text{cont}}}(m)
\end{aligned}$$

as $t \rightarrow \infty$ for some constant $\omega_\infty^{\text{cont}}$, which is the final consensus opinion.

Remark 3.12. Proving the convergence to the equilibrium for the continuum system is more challenging than in the discrete one. Notice that it is even not clear how to check that the limiting distributions are stationary solutions of the continuum equations (20a)–(20b) since one has to divide by $\int g(\omega, m) dm$.

Assuming the limits (27), it holds that

$$\int \int \omega g(\omega, m) \rightarrow \omega_\infty^{\text{cont}},$$

and by applying Lemma 3.10, the limiting value $\omega_\infty^{\text{cont}}$ is given by:

$$(28) \quad \omega_\infty^{\text{cont}} = \int \int \omega g(t=0, \omega, m) d\omega dm.$$

Finally, we notice that the limiting value $\omega_\infty^{\text{cont}}$ is the analogue to the discrete limiting value $\omega_\infty^{\text{micro}}$ in (3).

In conclusion, some structural properties of the discrete system investigated in Section 2.2 are captured by the continuum dynamics.

3.5. Conclusions from the basic continuum modeling framework. From the proposed modeling framework, we conclude that the continuum system (20a)-(20b) is well-suited for both numerical simulations and mathematical analysis. Numerical simulations will be presented in Section 5, while in the previous Section, we provided a basic mathematical analysis in the context of consensus dynamics, verifying that certain properties of the discrete system are preserved in the continuum model.

In this regard, we have successfully achieved our objective of developing an application-oriented framework for modeling continuum equations in opinion dynamics. However, an important limitation remains: we have not rigorously derived these continuum equations from the discrete system. Instead, we constructed the model using inspiration from mean-field approximations. Notably, Lemma 3.2 loses validity as $N \rightarrow \infty$, which can result in a loss of crucial network information in the continuum limit, as illustrated in Figure 3. To address this issue, we propose remedies in the following Section. These remedies involve augmenting the system with additional information to retain the network structure. However, this comes at the cost of increased complexity, potentially making the system less tractable for both analysis and simulation.

4. CONTINUUM MODELING FRAMEWORK: REFINEMENTS

The regime of validity of Lemma 3.4. In this article, we have relied on the validity of Lemma 3.4, which establishes the equivalence between the original discrete system (1) and the unlabeled model (13). For finite N , this equivalence holds, provided that $\omega_i(t) \neq \omega_j(t)$ for all $i, j = 1, \dots, N$ over some finite time interval. In other words, the equivalence is preserved as long as individuals can be distinguished by their opinions.

To overcome the challenge of indistinguishable individuals (i.e., when $\omega_i(t) = \omega_j(t)$ for some $i \neq j$), additional information can be introduced into the system. In the original paper [26], which inspired our derivation, the authors considered a system of particles defined by their positions and orientations. In that framework, particles interact only when they are spatially close, and spatial repulsion prevents them from overlapping, allowing them to remain distinguishable by using the information of their positions.

In our case, where spatial variables are absent, we can introduce an alternative form of distinguishing information. For example, instead of tracking only an agent's opinion $\omega_i(t)$ at time t , we could also track their initial opinion $\omega_i(0)$. This way, if the opinion of two agents overlap at some time t , they can still be distinguished by their distinct initial opinions.

Consequently, the continuum dynamics would give the evolution of the opinion distribution $f = f(t, \omega, \omega_0)$, which gives the density of agents with opinion ω at time t who initially held opinion ω_0 at time $t = 0$. Similarly, the edge distribution would be given by $g = g(t, \omega, \omega_0, m, m_0)$, representing the proportion of edges between agents with opinions ω and m at time t who initially had opinions ω_0 and m_0 , respectively (see remark 4.3 below for more details).

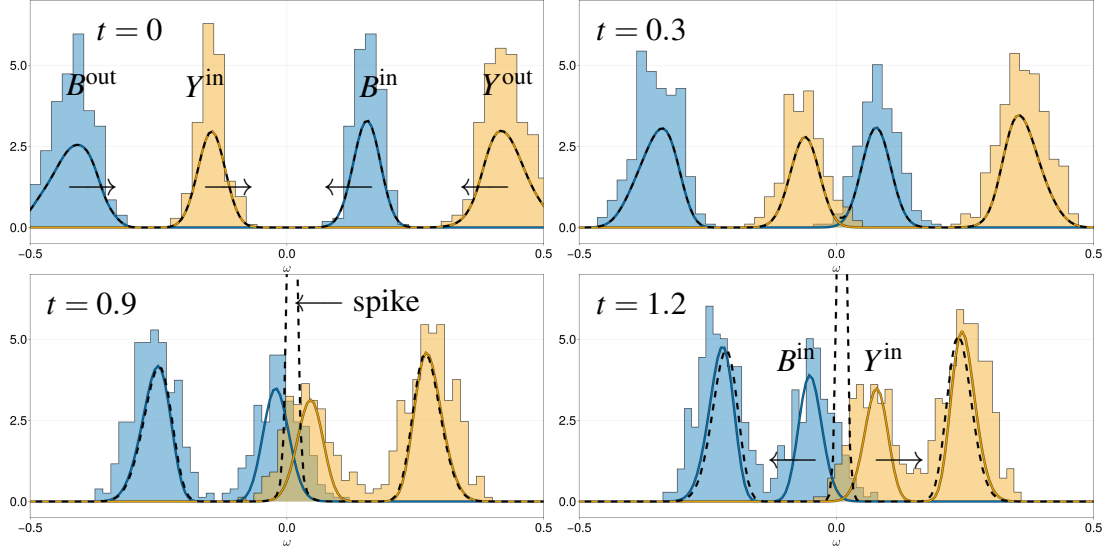


FIGURE 3. **Comparison between the discrete dynamics (histograms), the continuum model without group labeling (dash line) and the continuum model with group labeling (solid line).** The population is split in two groups, Blue and Yellow. The histogram represents the evolution of the discrete solution, while the dashed line is the solution to the continuous model without group labeling. The two groups are poorly connected to each other (the mixing parameter is $\mu = 1/20$, in other words, each individual has only $1/20^{\text{th}}$ of its connections to a group different from its own). The initial distribution in each group is not homogeneous, and consist of two subgroups denoted *in* and *out* respectively. Within a given group, as the agents are well connected, the distribution homogenizes quickly. Initially, there is a good agreement between the discrete and continuous opinion distributions, but starting at around $t = 0.3$, there is an overlap between subgroups B^{in} and Y^{in} . This is not captured correctly at the continuous level without group labeling: the subgroups merge and stop drifting around the origin, leading to a stable spike in the distribution, whereas they cross and separate in the microscopic model. The colored, solid lines correspond to a continuous model with group labeling presented in Section 4. This model captures well the discrete dynamics. For this plot, $N = 1000$.

While this approach preserves the ability to distinguish individuals, it comes at the cost of increasing the dimensionality of the system, thereby making computations significantly more costly.

Incorporating community structure. To simplify the problem and facilitate numerical testing, we propose a different approach: incorporating community information. Specifically, we assume the social network follows an LFR-type structure, where individuals are divided into $n > 0$ communities. Each agent i is represented by the pair (ω_i, p_i) , where ω_i is the agent's opinion and p_i is a community label, which is time-independent. The opinion dynamics remain the same as in equation (1), while the community label evolves trivially as

$$\frac{dp_i}{dt} = 0.$$

With this modification, we define the empirical opinion density and the edge distribution as:

$$(29) \quad f^N(t, \omega, p) := \frac{1}{N} \sum_{i=1}^N \delta_{(\omega_i(t), p_i)}(\omega, p),$$

$$(30) \quad g_r^N(t, \omega, p, m, q) := \frac{r^2}{2\mathcal{K}} \sum_{i \sim j} \delta_{(\omega_i(t), p_i)}(\omega, p) \delta_{(\omega_j(t), p_j)}(m, q),$$

where p and q are community labels.

To distinguish individuals with the same opinion but different group memberships, we define the distance between two individuals (ω, p) and (m, q) as:

$$\|(\omega, p) - (m, q)\| = |\omega - m| + |p - q|.$$

We impose the following assumption on the initial configuration:

Assumption 4.1. *There exists $r = r(N) > 0$ such that*

$$\inf_{i \neq j} \|(\omega_i(0), p_i) - (\omega_j(0), p_j)\| > 2r(N) > 0.$$

Under this assumption, we can extend the results of Lemma 3.4. Specifically, we have:

Lemma 4.2. *Under assumption 4.1 there exists $T > 0$, such that for all $t \in [0, T]$, the discrete system of equations (1) is equivalent to:*

$$(31) \quad \frac{d\omega_i(t)}{dt} = a[g_r^N](\omega_i(t), p_i) + B_r^{(N)}(\omega_i(t), p_i),$$

where $B_r^{(N)}(\omega_i(t), p_i) \rightarrow 0$ as $r \rightarrow 0$ for fixed N , and

$$(32) \quad a[g^N](\omega_i, p_i) := \sum_{q=1}^n \int \mathbf{D}(\omega_i - m) \eta^N(t, \omega_i, p_i, m, q) dm,$$

$$(33) \quad \eta^N(t, \omega, p, m, q) := \frac{g^N(t, \omega, p, m, q)}{\sum_{q=1}^n \int g^N(t, \omega, p, m, q)},$$

with $\eta[g](\omega, p, \cdot, \cdot) = 0$ if $g(\omega, p, \cdot, \cdot) = 0$ a.e.

Following analogous assumptions and procedure, we derive the continuum equations for (31):

$$(34) \quad \partial_t f(t, \omega, p) + \partial_\omega (a[g](\omega, p) f(t, \omega, p)) = 0,$$

$$(35) \quad \partial_t g(\omega, p, m, q) + \partial_\omega (a[g](\omega, p) g(\omega, p, m, q)) + \partial_m (a[g](m, q) g(\omega, p, m, q)) = 0,$$

$$(36) \quad a[g](\omega, p) f(t, \omega, p) = 0 \quad \omega \in \partial\Omega,$$

$$(37) \quad a[g](\omega, p) g(\omega, p, m, q) = 0 \quad (\omega, m) \in \partial\Omega^2.$$

These equations are structurally equivalent to the original system (20a)-(20b), but the functions f and g now depend on the additional variables p and (p, q) . This seemingly minor modification significantly increases the computational complexity.

For example, in our numerical simulations with n communities, we must compute n functions for the opinion density $f(t, \omega, p)$ (one for each group) and n^2 functions for the edge distribution $g(t, \omega, p, m, q)$, corresponding to all pairs $p, q \in \{1, \dots, n\}$. In contrast, the original system only required solving two equations, highlighting the increase in complexity from 2 to $n + n^2$ equations.

Remark 4.3. If we had chosen to track the initial opinions ω_0 and m_0 instead of community labels, the resulting continuum system would still correspond to (34)–(37), but having ω_0 instead of p and m_0 instead of q . But notice that ω_0 and m_0 take continuous values in Ω : this dramatically increases the computational cost, as opposed to handling discrete community labels p and q .

Conclusion: tailoring modeling choices. We conclude this Section by emphasizing that the continuum modeling framework must often be tailored to the specific system under consideration. Depending on the application, additional information such as community structure, initial data, or other distinguishing variables may need to be incorporated to accurately capture the network’s dynamics. These modifications, while necessary, increase the complexity of both the mathematical model and its numerical implementation.

5. NUMERICAL COMPARISON: CONSENSUS DYNAMICS BETWEEN THREE COMMUNITIES

This Section is dedicated to numerical experiments for both the discrete model of Section 2 and the continuous system of Section 2.2.2. We start by giving some details about the discretization, both in time and in opinion space, followed by considerations about the choice of initial data, and conclude by a comparison of both models for specific choices for the Lancichinetti–Fortunato–Radicchi (LFR) network [54], explained below.

5.1. Discretization.

The discrete model. We consider (1) with a fixed number of agents N on a given graph, described by the adjacency matrix A . For the time integration, we use a modified explicit Euler scheme: let $\Delta t > 0$ be the (fixed) time-step, and let $t_n = n \Delta t$, $n \in \mathbb{N}_{\geq 0}$ be the corresponding discrete times. We can then define the time-discrete opinions as

$$\omega_i^n := \omega_i(t = t_n) \quad 1 \leq i \leq N.$$

Equation (1) is then integrated in time using

$$(38) \quad \omega_i^{n+1} = \omega_i^n + \Delta t \frac{1}{\#\mathcal{J}_i} \sum_{j \in \mathcal{J}_i} \mathbf{D}(\omega_i^n - \omega_j^n),$$

where Δt must be chosen small enough to guarantee $\omega_i^{n+1} \in \Omega$, regardless of Assumptions 2.2. More precisely, if $\Delta t \leq \|\partial_z \mathbf{D}\|_{L^\infty}^{-1}$, one can prove that ω_i^{n+1} is in the convex hull of $\{\omega_i^n\} \cup \{\omega_j^n : j \in \mathcal{J}_i\}$, and in particular $\omega_i^{n+1} \in \Omega$. For details, see e.g. Appendix B.

The continuum system. We now turn to the system (21), which we solve using an adaptation of the classical local Lax-Friedrich (LLF) finite volume scheme [57]. The Lax-Friedrich method was initially proposed to approximate solutions of hyperbolic, linear conservation laws, later generalized to the nonlinear case, that is to equations of the form

$$(39) \quad \partial_t q + \partial_\omega(b(q(\omega))) = 0, \quad \omega \in \Omega,$$

there the flux function b is a function of *pointwise* values of the unknown q , which makes the equation *local*. Although it is only first order accurate and suffers from high numerical diffusion, it is conservative and is relatively easy to extend.

System (21) falls out of the scope of the LLF method for at least two reasons: first, it is a system of two equations, one set on Ω and coupled, through the factor $a[g]$, to the other, which is set on $\Omega \times \Omega$. Second, not only are these equations nonlinear, but the flux $\omega \mapsto a[g](\omega)f(\omega)$ is not a function of $f(\omega)$ alone. It depends *non locally* on g , and is *space varying*. The integral factor $a[g]$ thus introduces space dependence, coupling and non locality.

The LLF scheme also covers non-constant flux functions, so the first point is not a problem. We can deal with the second point by neglecting the dependency of $a[g]$ on g , i.e. by first fixing a , then solving (20a) and (20b) independently at each time-step with the LLF scheme and finally updating a . This way, we are back in the linear setting.

More precisely, we fix the discretization with $N_{\text{cont}} > 0$ and define $\Delta x = |\Omega|/N_{\text{cont}}$. For $0 \leq i \leq N_{\text{cont}} - 1$, define the finite volumes $I_i = [-1 + (i + 1/2)\Delta x]$ and integrate (20a) on I_i to get

$$\frac{d}{dt} \int_{I_i} f + \int_{\partial I_i} a f = 0.$$

For some measurable set B , we define the average $f|_B = \int_B f / |B|$, so that we can now take the piecewise constant approximation of f , $f_i := f|_{I_i}$. Now, a_i is defined similarly, by averaging $a[g]$. This yields

$$(40) \quad \frac{d}{dt} \int_{I_i} f_i + \widehat{a} f_{i+1/2} - \widehat{a} f_{i-1/2} = 0,$$

where $\widehat{a} f_{i\pm 1/2}$ is the so-called numerical flux, which takes the place of the (ill-defined) boundary terms. Likewise for equation (20b), we get the following integrated equation for $g_{i,j}$:

$$(41) \quad \frac{d}{dt} \int_{I_i \times I_j} g_{i,j} + \widehat{a} g_{i+1/2,j} - \widehat{a} g_{i-1/2,j} + \widehat{a} g_{i,j+1/2} - \widehat{a} g_{i,j-1/2} = 0.$$

We take the local Lax-Friedrich flux, which in our case is given by

$$\widehat{a} f_{i+1/2} = \frac{1}{2} (a_i f_i + a_{i+1} f_{i+1} - (f_{i+1} - f_i) \max(|a_i|, |a_{i+1}|)).$$

Here, we have neglected the dependence of a on the pointwise value of f on I_i , which is reasonable for large values of N_{cont} . We can use a similar approach for g with:

$$\widehat{a} g_{i+\frac{1}{2},j} = \frac{1}{2} \left(a_{i,j} g_{i,j} + a_{i+\frac{1}{2},j} g_{i+\frac{1}{2},j} - (g_{i+\frac{1}{2},j} - g_{i,j}) \max(|a_i|, |a_{i+1}|) \right)$$

and $\widehat{af}_{i-\frac{1}{2}}$, $\widehat{ag}_{i-\frac{1}{2},j}$, $\widehat{ag}_{i,j+\frac{1}{2}}$ and $\widehat{ag}_{i,j+\frac{1}{2}}$ are defined likewise.

The boundary conditions (21a)-(21b) are enforced by setting

$$\begin{aligned}\widehat{af}_{-1/2} &= \widehat{af}_{N_{\text{cont}}+1/2} = 0, \\ \widehat{ag}_{-1/2,j} &= \widehat{ag}_{N_{\text{cont}}+1/2,j} = \widehat{ag}_{i,-1/2} = \widehat{ag}_{j,N_{\text{cont}}+1/2} = 0.\end{aligned}$$

We then discretize (40) and (41) in time with time-step Δt to get

$$\begin{aligned}f_i^{n+1} - f_i^n &= -\frac{\Delta t}{\Delta x} \left(\widehat{af}_{i+1/2}^n - \widehat{af}_{i-1/2}^n \right), \\ g_{i,j}^{n+1} - g_{i,j}^n &= -\frac{\Delta t}{\Delta x} \left(\widehat{ag}_{i+1/2,j}^n - \widehat{ag}_{i-1/2,j}^n \right. \\ &\quad \left. + \widehat{ag}_{i,j+1/2}^n - \widehat{ag}_{i,j-1/2}^n \right),\end{aligned}$$

where, as above, the exponent n indicates the approximation at time $t^n = n\Delta t$.

Remark 5.1. This numerical scheme is extended in a straightforward manner when we consider the continuum equations containing the group labels (34)-(37).

5.2. Choice of the network and initial opinion distribution. The specific choice of initial opinion distribution and more importantly the choice of the network will depend on the real system being modelled. There are many possibilities to do that, and it is out of the scope of the present paper to review them. We will focus on interactions between communities using the LFR network.

Since our goal here is to assess the continuous system's ability to approximate the discrete model, we construct the initial data of the continuous system from that of the discrete as follows:

- (1) fix the number of agents N for the discrete equation (1) and the discretization size N_{cont} for the continuous system (21);
- (2) pick an initial opinion distribution f_0 and a network G of size N ;
- (3) construct the initial opinions $(\omega_i^0)_{1 \leq i \leq N}$ by sampling f_0 ;
- (4) compute the initial discrete distribution $(f_i^0)_{1 \leq i \leq N_{\text{cont}}}$ by averaging f_0 over I_i ;
- (5) compute the initial discrete distribution $(g_{i,j}^0)_{1 \leq i,j \leq N_{\text{cont}}}$ by kernel density estimation (KDE) of $g^N(t=0)$ as defined in (9) and averaging over $I_i \times I_j$. The kernel bandwidth is taken equal to the (one-dimensional) Sheather-Jones bandwidth [68] corresponding to ω_i^0 . We use the KDE as a black box to get a continuous approximation of the sum of Dirac deltas. We refer the interested reader to Chen's[21] introduction to the method.

For the choice of network, we are particularly interested in how the presence of communities affect the agreement between both models. For this, we consider graphs and opinion distributions initially displaying some amount of so-called homophily. That is: clusters in the network structure corresponding to localized bumps in the opinion distribution, and vice versa. By

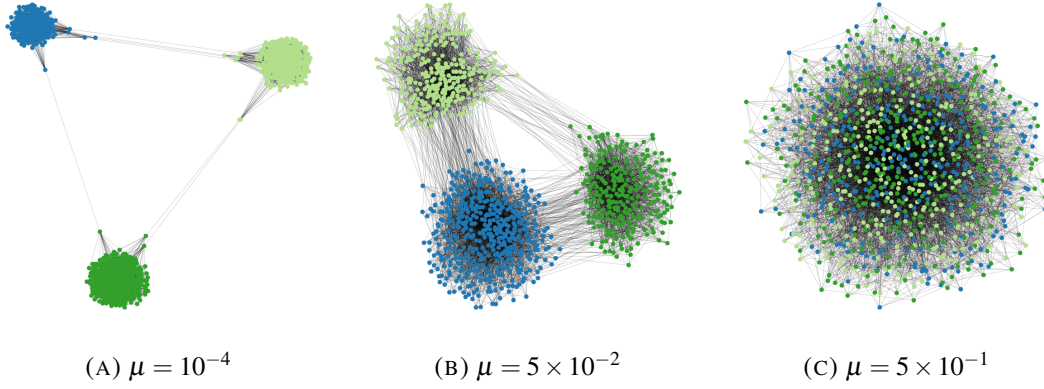


FIGURE 4. Typical LFR graphs for selected values of the mixing parameter μ . We did not include the case $\mu = 1$ as it is visually similar to that of $\mu = 0.5$.

changing how isolated the clusters are within the network and how localized the opinions are within these clusters, one we construct different initial conditions.

In practice, we use Lancichinetti–Fortunato–Radicchi’s algorithm[54] to generate graphs, where each node (or individual) i is assigned to a community $c(i) \in \{1, 2, 3\}$. Within each of these communities, the initial distribution of opinion is similar to that of Figure 3. More precisely, the initial distribution is a weighted sum of normal distributions, centered on $-1/2$ and $1/4$ for community 1, 0 for community 2, and $-1/4$ and $1/2$ for community 3, with the *outer* normal components (those centered on $-1/2$ and $1/2$) having a higher weight and variance than the *inner* ones. This is arguably an artificial setup, but it helps to highlight the impact of introducing group labeling in the continuous model; this will become clearer below. Communities do not have equal sizes in general, and since the opinion distribution is weighted by community size, one cannot expect the overall distribution to be even as a function. The overall initial distribution f_0 is then a weighted sum of five truncated normal distributions, weighted by community size. The corresponding initial opinion distributions are shown in Figure 5.

We vary the mixing parameter μ of the LFR algorithm: for $\mu = 0$, individuals are connected to individuals within the same community, whereas for $\mu = 1$, they are connected only to individuals outside their own. Some typical network topologies corresponding to $\mu \in \{10^{-3}, 5 \times 10^{-2}, 5 \times 10^{-1}, 1\}$ are shown in Figure 4.

The impact of the value of μ is reflected in the initial profile for g , which is presented in Figure 6. For large μ (right), all subgroups are connected to each other: for any two ω, ω' such that $f(\omega) > 0$ and $f(\omega') > 0$ we have that $g(\omega, \omega') > 0$. As μ decreases (going to the left), these links “fade”: the corresponding $g(\omega, \omega')$ decreases until it reaches 0 if (ω, ω') do not correspond to positive densities in a single subgroup. We underline that, in all cases, we consider connected graphs.

5.3. Results. Here we present selected results, comparing the discrete and the continuous models on the LFR generated graphs.

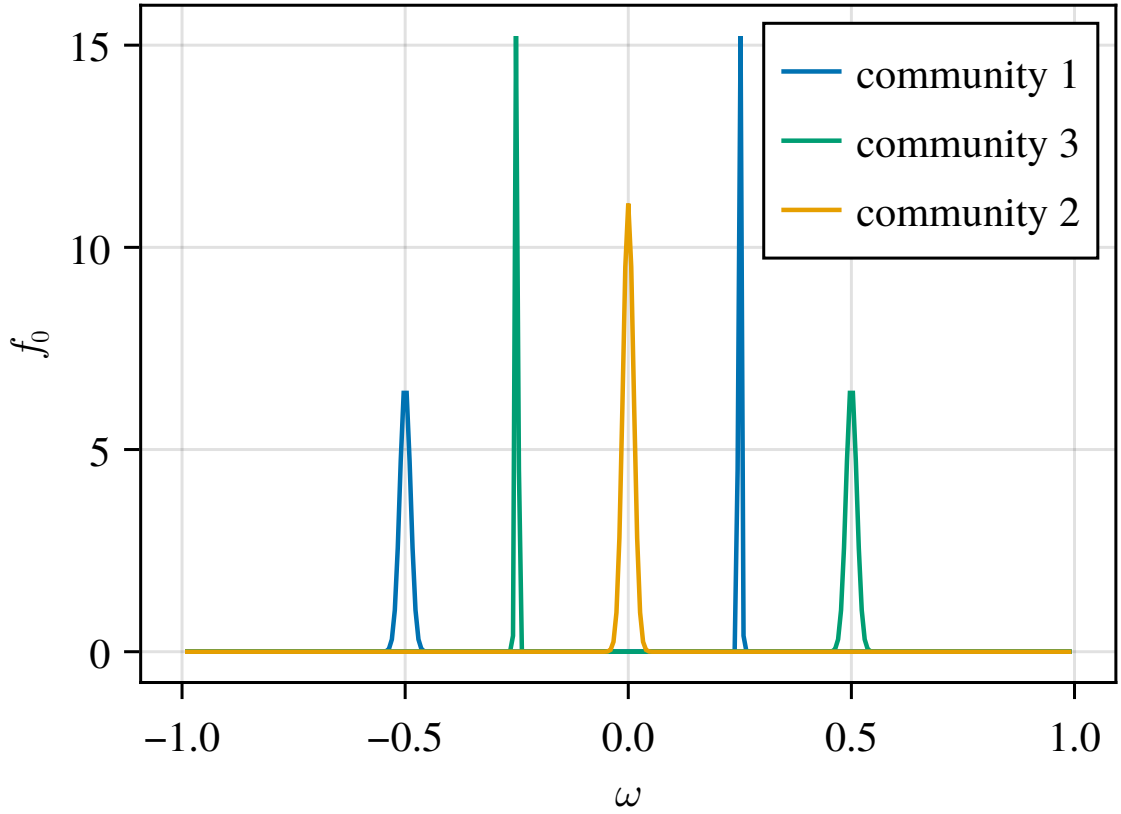


FIGURE 5. Initial opinion distribution, assuming three communities of identical size. Each color corresponds to a community.

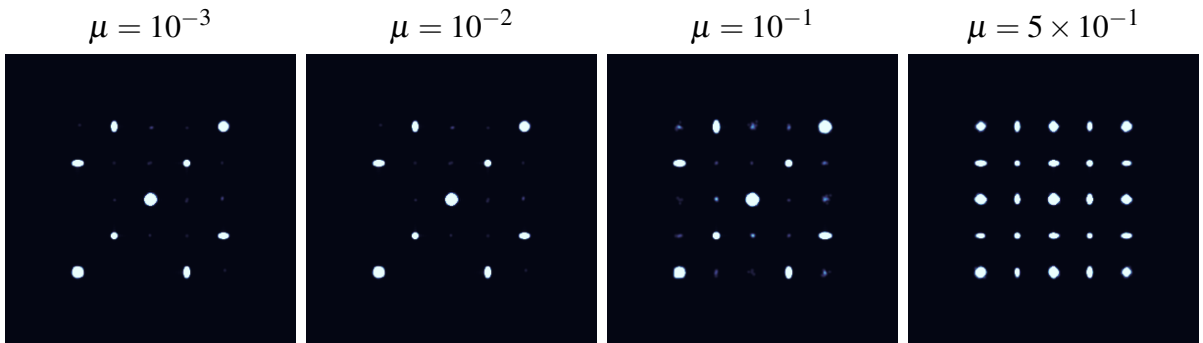


FIGURE 6. Density plots for a typical initial value of g . The lighter the color is, the higher the density is. The value μ is the mixing parameter of the LFR graph (see Fig. 4).

The computations were carried out with $N = 1000$ agents for the discrete model and a discretization size of $N_{\text{cont}} = 303$ for the continuous system. With our choice of parameters, the average degree of nodes is 15 and $\kappa \sim 1.5 \times 10^4$, so that the fill-ratio of the adjacency matrix is roughly 1.5%. Notice that with these values for N and κ , the graph is sparse[28]. We choose $\mathbf{D}(z) := -z$, so that we have the rough estimate $|a[g]| \leq 2$, thus the CFL condition associated to the LLF scheme is $\Delta t < \frac{1}{2}\Delta x = N_{\text{cont}}^{-1} \simeq 3 \times 10^{-3}$. This leads us to the choice $\Delta t = 10^{-3}$.

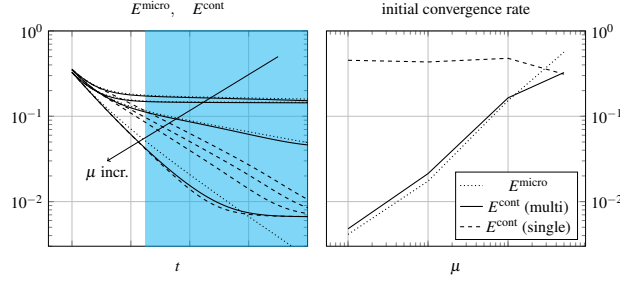


FIGURE 7. Convergence rates as a function of the mixing parameter μ .

Comparison of the convergence to the consensus value ω_∞ . Because we only consider connected graphs, we expect convergence to consensus in all cases, for both the discrete and continuous models. The consensus opinion is given by $\omega_\infty^{\text{micro}}$ and $\omega_\infty^{\text{cont}}$, given by (3) and (28). Both coincide, theoretically, as $N \rightarrow \infty$. Because of the sampling required at initialization, there is no reason to expect the two to be equal.

To compare the two models quantitatively, we rather focus on the speed of convergence to consensus in terms of the ℓ^2 (resp. L^2) distance to $\omega_\infty^{\text{micro}}$ (resp. $\omega_\infty^{\text{cont}}$):

$$E^{\text{micro}}(t) = \left(\frac{1}{N} \sum_i (\omega_i(t) - \omega_\infty^{\text{micro}})^2 \right)^{\frac{1}{2}},$$

$$E^{\text{cont}}(t) = \left(\sum_p \int (\omega - \omega_\infty^{\text{cont}})^2 f(t, \omega, p) d\omega \right)^{\frac{1}{2}}.$$

In view of Proposition 2.6, we expect exponential convergence of E^{micro} to zero.

Exponential convergence rates and numerical diffusion. As was already mentioned, the LLF scheme suffers from numerical diffusion, which means that we cannot expect E^{cont} to vanish but rather to converge to a positive constant, as $t \rightarrow \infty$, something which is confirmed by the plots in Figure 7 (left): E^{cont} decreases but remains roughly above 7×10^{-3} .

To have a quantitatively meaningful comparison, we estimated the exponential convergence rates for both E^{micro} and E^{cont} in the interval $t \in [2, 8]$, in which the effect of the numerical diffusion is only significant for the largest value of μ (0.5). There is a transient relaxation phase where the convergence is not exponential (as evidenced by the strictly convex profiles on the left of Figure 7). This motivates the restriction to $t \in [2, 8]$ for the estimation of the convergence rate. In practice, we perform a linear regression between t and $\log E^{\text{micro}}$ (resp. E^{cont}). The fit of this linear regression is very good: for over 500 sampling points, the average fit error is below 5% for $\mu = 0.5$, and below 1% otherwise. These convergence rates are shown in Figure 7 (right) and the corresponding time interval has been shaded in blue (left).

Observations. We observe that the rate of convergence increases for increasing values of the connectivity parameter μ for both the discrete and continuous models. This is not surprising as

a larger value of μ implies increasing connectivity between different groups, particularly, for $\mu = 0.5$ one cannot see distinct groups graphically in Figure 4.

We observe that for small μ there is a good agreement between the discrete model (DM) and the continuous model with group labeling (CML). In contrast, the continuous model with no group labeling (CMnoL) does not capture the rate of convergence of the microscopic dynamics. In particular, the estimated convergence rate for CMnoL is practically constant in μ . This indicates that the refinement of CMnoL to CML is necessary to obtain the right approximation in the limit $N \rightarrow \infty$.

For $\mu = 0.5$, CML and CMnoL behave similarly, the convergence seems faster than for DM initially, but then slows down until E^{cont} plateaus. This is also visible on the right of Figure 7, where the estimated convergence rates for CML and CMoL is lower than that of DM. The main cause is the diffusivity of the numerical scheme used for the continuous models, and does not reflect an issue with the models themselves. Actually, for this value of μ , the error between DM and CMnoL is the smallest. This can be explained, as we mentioned above, by the fact that there are not clear distinct groups in this situation, so adding group labeling does not provide much additional information.

Qualitative comparison. The simulations carried out to compute the convergence graph in Figure 7 can be found in Figshare in the form of videos:

dx.doi.org/10.6084/m9.figshare.28023551

We can observe qualitatively that the continuous model with group labeling approximates well the discrete dynamics even in the case $\mu = 0.5$; and that the continuous model without group labeling clearly fails in all cases except when $\mu = 0.5$. We notice also that the case $\mu = 0.5$ stands out, as there is no crossing of bumps between the green and blue groups.

Interpretation. In this Section, we explain why the continuous model with group labeling has a good match with the discrete dynamics while the model with no group label fails to do so. We illustrate this with a simple example in Figure 8, where we suppose that our initial datum describes 2 communities. Within each community, the opinion is distributed in two peaks around two mean opinions: one main group around M_i , and a smaller one around m_i . We suppose individual A from community 1 (the blue one in Figure 8) has opinion ω_A^1 and individual B from community 2 (the orange one in Figure 8) has opinion ω_B^2 . Their opinion are such that they belong to the smaller groups, i.e. they are such that

$$M_1 < \omega_B^2 \simeq m_2 < m_1 \simeq \omega_A^1 < M_2.$$

By construction, A has more connections with community 1, at initial time its opinion will relax towards M_1 , while for individual B , its opinion will relax towards M_2 (this motion is represented by the arrows in Fig. 8a). This means that, by continuity, there is a time t in which $\omega_A^1(t) = \omega_B^2(t)$ (see Fig. 8b). At this point, it is not possible to distinguish the communities, since the opinions

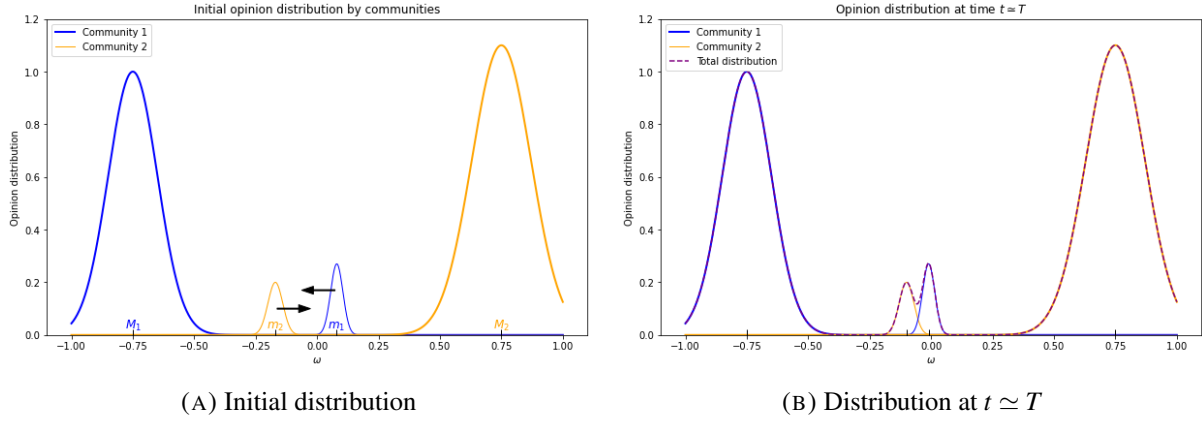


FIGURE 8. Overlap of communities opinion distribution.

overlap. When the opinions overlap, Lemma 3.2 is violated and the network described by g may lose its capacity to represent the original underlying discrete network. However, when we add the group label, we are able to distinguish between two overlapping opinions and g can now describe with accuracy the underlying network. This effect can also be visualized in Fig. 3.

To conclude, the numerical simulations indicate that the continuum model with group labeling can be used to investigate the interaction between different communities that initially have non-overlapping opinions with other communities.

5.4. Implementation and code. The numerical methods presented above are implemented in Julia, using the following packages: `Distributions.jl`[12], `Graphs.jl`, `GraphMakie.jl`[36], `KernelDensity.jl`, `Makie.jl`[23], `LFRBenchmarkGraphs.jl`[38], `ShiftedArrays.jl`, `SparseArrays.jl`, `SpecialFunctions.jl`. The code is available at:

<https://github.com/gjankowiak/OpiForm>.

6. EXTENSIONS OF THE MODELING FRAMEWORK TO OTHER TYPES OF NETWORKS

The continuum model proposed here is a basic model upon which more complex features can be built. This is one important reason why we proposed this model in contrast to other existing large-particle limit for networks, like graphons. Particularly, there are some important features that can be easily incorporated. We discuss them next.

6.0.1. Random creation and destruction of edges (dynamical networks). In the spirit of [25], one can consider a system where a new edge is created at rate λ between agent i with opinion ω and agent j with opinion m ; or that an edge between ω and m is destroyed at rate μ . These dynamics would result in an additional term on the right-hand-side of equation (20b) for g , of the form:

$$\lambda f(\omega)f(m) - \mu g(\omega, m).$$

This reflects the fact that two opinions ω and m create a new edge at rate λ with a probability given by the proportion of individuals with opinion ω and m , i.e, with a probability $f(\omega)f(m)$; at the same time, an existing edge between opinions ω and m is destroyed at rate μ with a probability given by $g(\omega, m)$, i.e., the proportion of edges that exist between opinions ω and m .

One can consider different creation probabilities like, for example, a probability that takes into account the number of intermediate nodes connecting ω and m . In this case we will have a creation term of the form

$$\lambda \left(\int g(\omega, u)g(u, m)du \right) f(\omega)f(m).$$

In another variant, one can consider that edge creation depends on the connectivity of opinion m (where the connectivity corresponds to $\int g(\omega, m) dm$), for example, the more connected an opinion is, the more edges are created around that opinion. In this case, we can consider a creation term of the form

$$\lambda \phi[g](\omega, m) f(g)f(m),$$

where

$$\phi(g) := H(\max\{\int g(\omega, u)du, \int g(m, u)du\})$$

for some increasing function H .

One can also consider destruction of edges based on the distance between the opinions. For example, the further opinions are, the easier is to break the edge between them. In this case, one can consider a destruction term of the form

$$-\mu H(|\omega - m|)g(\omega, m),$$

for H increasing.

6.0.2. Noise at the particle level. One can consider a stochastic differential version of our original system of ODEs (1):

$$(42) \quad d\omega_i(t) = \frac{1}{\#\mathcal{I}_i} \sum_{j \in \mathcal{I}_i} \mathbf{D}(\omega_j(t) - \omega_i(t)) dt + \sqrt{2\sigma} dB_t^i,$$

where $\sigma > 0$ is the diffusive constant and $(B^i)_{i=1, \dots, N}$ are independent Brownian motions. If \mathbf{D} is globally Lipschitz (which is the case of consensus dynamics that we considered here), then we have existence and uniqueness of solutions (pathwise and in law) for (42). This would modify (formally) the continuum equations, for the opinion distribution

$$\partial_t f(\omega) + \partial_\omega (a[g](\omega)f(\omega)) = \sigma \partial_\omega^2 f(\omega), \quad \omega \in \Omega,$$

and for the connectivity

$$\begin{aligned} \partial_t g(\omega, m) + \partial_\omega (a[g](\omega)g(\omega, m)) + \partial_m (a[g](m)g(\omega, m)) \\ = \sigma (\partial_\omega^2 + \partial_m^2) g(\omega, m), \quad (\omega, m) \in \Omega^2, \end{aligned}$$

where the Laplacian for the equation of g is a consequence of Itô's Lemma (and adding boundary conditions to have zero flux at the boundary).

Adding diffusion to the dynamics is used to represent self-thinking or changes in opinion due to interactions with the media (which is outside the network), see e.g. [13].

6.0.3. *Directional network.* We considered undirected networks, but one can extend this analysis to directional networks. The big difference concerns the definition of g^N in (9) which would no longer be symmetric and would be given by

$$g^N(t, \omega, m) := \frac{1}{\kappa} \sum_{i \rightarrow j} \delta_{\omega_i(t)}(\omega) \delta_{\omega_j(t)}(m),$$

where $i \rightarrow j$ indicates that i influences (is connected to) j (but not the other way around). Then one needs to carry out the steps in Sections 3.2 and 3.3 paying attention to the lack of symmetry of the interactions.

6.0.4. *Non-weighted interactions.* One can consider the discrete system (1) without the weights $\#\mathcal{S}_i$. Also in this setup, one can carry out the analysis as done previously, but the discrete system (1) needs then to be rescaled. This corresponds to mean-field limits, where the forces (the right-hand-side of (1)) are rescaled by a multiplying factor $1/N$ [19, 20]. Since we are not working with a mean-field force, but with a network-mediated force, the analogue of this would be to rescale the force by a multiplying factor proportional to $1/\kappa$.

7. CONCLUSIONS AND PERSPECTIVES

In this paper, we propose a framework for the continuum modeling of opinion dynamics on networks. Our primary objective is to develop a continuum representation that is both amenable to numerical simulation and rigorous mathematical analysis, making it suitable for practical applications.

We illustrated this framework on a system formed by a fixed undirected network, where individuals undergo pairwise interactions with those individuals with whom they are connected. For this system, we proposed the continuous model (21) as an approximation of the discrete model (1). The key for its derivation is to obtain a description of the network that does not use the labels of the individuals.

We compared numerically the discrete and continuous models in a setup of consensus dynamics between three communities, and we observed that the continuous model with group labelling gives a good match with the discrete dynamics while the continuous models without group labeling fails in general to do so. The numerical implementation required various approximations, and more efficient and accurate methods to simulate the continuum dynamics would be required for more complex setups.

7.0.1. *Applications.* The goal of the proposed framework is to obtain continuum equations that are amenable to investigating opinion dynamics on social networks. For example, as a future perspective, one could investigate reported social effects like epistemic bubbles and echo chambers [60]. These concepts are used in sociology to explain opinion segregation and polarization via the interaction between communities. We do not dwell here on these concepts, but stress that they have become important in social sciences:

“While online echo chambers and epistemic bubbles are commonly found on social media sites like Twitter and Facebook, they are not restricted to such digital platforms. Any online space where information is shared has the potential to become an echo chamber or epistemic bubble. Examples include online forums (e.g., Reddit and Quora), news blogs, video-sharing platforms, online gaming communities, online marketplaces, and review sites.” (Turner, 2023[73])

7.0.2. *Open problems.*

The validity of assumption 3.1 as $N \rightarrow \infty$. As $N \rightarrow \infty$ the conditions for Lemma 3.4 to hold fall apart since there is no $r > 0$ for which (8) holds as $N \rightarrow \infty$. The hope, though, is that the continuum equations provide a good approximation of the discrete ones. For the moment, we can test this only numerically. It will be the issue of future investigation to find a correct analytic measurement to quantify how good is the continuum approximation.

Conditions for the limiting network to exist and rigorous mean-field limit. A fundamental question is how a network should scale as $N \rightarrow \infty$ for the continuum equations to make sense. In other words, we require that the initial edge distribution $g^N|_{t=0}$ admits a well-defined limit as $N \rightarrow \infty$. What assumptions on $g^N|_{t=0}$ are necessary to guarantee the existence of this limit? This is a challenging open problem. In works such as [64], the existence of this limit is assumed.

Even if this limit exists, rigorously proving the convergence of f^N and g^N to their respective continuum counterparts as $N \rightarrow \infty$ (Assumption 3.6) remains a significant challenge [19, 20]. Ideally, one would also like to derive an analytical estimate of the convergence rate of the discrete system to the continuum system for large values of N , similar to what is achieved in classical mean-field limits [71, 18].

Numerical methods. As mentioned in Section 4, refinements of the basic framework may be needed to capture well the network structure. These refinements require adding more information in the system, which increases its computational cost. A future problem will be how to find efficient numerical methods for some of these refinements.

Acknowledgment. The authors thank Pierre Degond (CNRS, University of Toulouse) and Antoine Diez (University of Kyoto) for useful discussions and tips. GF has been partially financed by the Austrian Science Fund (FWF) project 10.55776/F65, by INdAM | Gruppo Nazionale per l’Analisi Matematica, la Probabilità e le loro Applicazioni (INdAM/GNAMPA) no. E55F22000270001 and no. E53C22001930001. GF also wants to thank the Department of

Applied Mathematics and Mathematical Physics of the Urgench State University. The work of SMA was funded by the Vienna Science and Technology Fund (WWTF) [10.47379/VRG17014].

APPENDIX A. EXPONENTIAL CONVERGENCE TO CONSENSUS IN THE LINEAR CASE.

Here we sketch a proof of Proposition 2.6. In the case $\mathbf{D}(z) = -z$, our system of equations (1) is a linear ODE system of the form

$$\begin{cases} \frac{du(t)}{dt} = Qu(t) & t > 0, \\ u(0) = u_0 & t = 0, \end{cases}$$

where $u = (\omega_1, \dots, \omega_N)$ and the constant $N \times N$ matrix Q is given by

$$Q_{ij} = \begin{cases} -1 & \text{if } i = j, \\ (\#\mathcal{S}_i)^{-1} & \text{if } i \sim j. \\ 0 & \text{otherwise.} \end{cases}$$

One has $Q = M^{-1}A - I$, where I is the identity matrix and where $M := \text{diag}(\#\mathcal{S}_i)$ is the diagonal matrix whose i^{th} diagonal element is $\#\mathcal{S}_i$. With this definition, the matrix $L := -MQ = -Q^T M$ is called the *Laplacian matrix* of the graph in spectral graph theory:

$$L_{ij} = \begin{cases} \#\mathcal{S}_i & \text{if } i = j, \\ -1 & \text{if } i \sim j, \\ 0 & \text{otherwise.} \end{cases}$$

The matrix L , unlike Q , is symmetric. It holds that $L_{ii} = \sum_{j \neq i} |L_{ij}|$ and $Q_{ii} = -\sum_{j \neq i} |Q_{ij}|$. As a consequence, through Gershgorin's Disc Theorem[42], we know that their respective spectra, denoted by $\sigma(L)$ and $\sigma(Q)$, satisfy

$$\sigma(L) \in [0, 2 \max \#\mathcal{S}_i], \quad \text{Re}(\sigma(Q)) \in [-2, 0],$$

where Re denotes the real part. For L , the multiplicity of the eigenvalue 0 is given by the number of connected components of the graph. In our case the graph is connected, so 0 is a simple eigenvalue. Since $\ker L = \ker Q$, 0 is also a simple eigenvalue of Q . The corresponding eigenspace—the kernel—is given by $\text{span}(\mathbf{1}_n)$, where $\mathbf{1}_n = (1, \dots, 1)$, i.e. vectors whose entries are equal.

We can write u using a decomposition on the kernel and its orthogonal:

$$u = \tilde{u} + \omega_\infty^{\text{micro}} \mathbf{1}_n := (u - \omega_\infty^{\text{micro}} \mathbf{1}_n) + \omega_\infty^{\text{micro}} \mathbf{1}_n,$$

by construction, $\tilde{u}(t) \in \ker(Q)^\perp$ and $\omega_\infty^{\text{micro}} \mathbf{1}_n \in \ker(Q)$ for all t . It then holds

$$\frac{d\tilde{u}}{dt} = \frac{du}{dt},$$

again by construction. We can now show the exponential convergence of a weighted ℓ^2 -norm of \tilde{u} . We introduce the inner product $\langle \cdot, \cdot \rangle_M := \langle \cdot, M \cdot \rangle$, along with the associated norm, $\| \cdot \|_M$. Because $L = -MQ$ is symmetric, Q is self-adjoint with this inner product. We have

$$\begin{aligned} \frac{1}{2} \frac{d}{dt} \|\tilde{u}\|_M^2 &= \langle \tilde{u}, Q\tilde{u} \rangle_M = -\langle \tilde{u}, L\tilde{u} \rangle \leq - \min_{\lambda \in \sigma(L) \setminus \{0\}} \lambda \|\tilde{u}\|_M^2 \\ &\leq - \left(\min_{\lambda \in \sigma(L) \setminus \{0\}} \lambda \min_i \#\mathcal{S}_i \right) \|\tilde{u}\|_M^2. \end{aligned}$$

The first inequality follows from the fact that $\tilde{u} \in \ker(L)^\perp$. The second from the fact that $\#\mathcal{S}_i \geq 1$ by assumption. Gronwall's Lemma yields *exponential convergence* of $\|\tilde{u}\|_M$:

$$(43) \quad \|\tilde{u}(t)\|_M \leq \exp(-\alpha t) \|\tilde{u}_0\|_M,$$

where $\alpha = \min_{\lambda \in \sigma(L) \setminus \{0\}} \min_i \#\mathcal{S}_i$ is the exponential convergence *rate*. By the equivalence of norms, this also holds for the Euclidean norm $\| \cdot \|$ up to a multiplicative constant C .

APPENDIX B. STEP-SIZE FOR THE DISCRETE MODEL

In this Section, we investigate which condition on the step-size Δt is sufficient to get rid of the clamping function in (38). More precisely, we prove

Proposition B.1. *Consider a connected graph of size N , with opinions $(\omega_i)_{1 \leq i \leq N} \subset \Omega$ and $(\mathcal{S}_i)_{1 \leq i \leq N}$ defined as in Section 2. Let $\mathbf{D} : \mathbb{R} \rightarrow \mathbb{R}$ satisfying Assumption 2.2. For $1 \leq i \leq N$, define ψ_i*

$$\psi_i := \omega_i + \Delta t \frac{1}{\#\mathcal{S}_i} \sum_{j \in \mathcal{S}_i} \mathbf{D}(\omega_i - \omega_j).$$

If $\Delta t \leq \|\partial_z \mathbf{D}\|_{L^\infty}^{-1} = \|\partial_z^2 W\|_{L^\infty}^{-1}$, then $(\psi_i)_{1 \leq i \leq N} \subset \text{Conv}(\{\omega_i\} \cup \{\omega_j : j \in \mathcal{S}_i\})$, where $\text{Conv}(A)$ denotes the convex hull of the set A .

In particular, we have $(\psi_i)_{1 \leq i \leq N} \subset \Omega$.

Proof. We define $[c_i^{\min}, c_i^{\max}] := \text{Conv}(\{\omega_i\} \cup \{\omega_j : j \in \mathcal{S}_i\})$, so that we must show:

$$c_i^{\min} - \omega_i \leq \psi_i - \omega_i \leq c_i^{\max} - \omega_i, \quad \forall 1 \leq i \leq N.$$

We only deal with the lower bound (the left inequality), the upper bound can be shown in an identical way. First define $\underline{\mathbf{D}} : z \mapsto -\|\partial_z^2 W\|_{L^\infty} \max(0, z)$, which is non-increasing. We have

$$\begin{aligned} \mathbf{D}(\omega_i - \omega_j) &= \int_0^{\omega_i - \omega_j} \partial_z \mathbf{D}(z) dz = - \int_0^{\omega_i - \omega_j} \partial_z^2 \mathbf{W}(z) dz \\ &\geq \underline{\mathbf{D}}(\omega_i - \omega_j) \geq \underline{\mathbf{D}}(\omega_i - c_i^{\min}), \end{aligned}$$

using the fact that $\partial_z^2 W > 0$. Summing over $j \in \mathcal{S}_i$ and dividing by $\#\mathcal{S}_i$ we get

$$\Delta t \underline{\mathbf{D}}(c_i^{\min} - \omega_i) \leq \psi_i - \omega_i.$$

On the one hand, if $c_i^{\min} < \omega_i$, then $\mathbf{D}(\omega_i - c_i^{\min}) = \|\partial_z^2 W\|_{L^\infty}(c_i^{\min} - \omega_i) \leq 0$ and it follows

$$c_i^{\min} - \omega_i \leq \Delta t \|\partial_z^2 W\|_{L^\infty}(c_i^{\min} - \omega_i) \leq \psi_i - \omega_i.$$

On the other hand, if $c_i^{\min} - \omega_i = 0$, i.e. $\omega_i - \omega_j \leq 0$ for $1 \leq j \leq N$, then $0 \leq \mathbf{D}(\omega_i - \omega_j)$ and $c_i^{\min} - \omega_i = 0 \leq \psi_i - \omega_i$, which completes the proof. \square

REFERENCES

- [1] Robert P. Abelson. Mathematical models in social psychology. volume 3, pages 1–54. Academic Press, 1967.
- [2] R.P. Abelson. Mathematical models of the distribution of attitudes under controversy. In N. Fredericksen and H. Gullicksen, editors, *Contributions to mathematical psychology*. Holt, Rinehart & Winston, 1964.
- [3] Giacomo Albi, Lorenzo Pareschi, and Mattia Zanella. On the optimal control of opinion dynamics on evolving networks. In *System Modeling and Optimization: 27th IFIP TC 7 Conference, CSMO 2015, Sophia Antipolis, France, June 29-July 3, 2015, Revised Selected Papers 27*, pages 58–67. Springer, 2016.
- [4] Nathalie Ayi and Nastassia Pouradier Duteil. Large-population limits of non-exchangeable particle systems. 2024.
- [5] Nathalie Ayi and Nastassia Pouradier Duteil. Mean-field and graph limits for collective dynamics models with time-varying weights. *Journal of Differential Equations*, 299:65–110, 2021.
- [6] Julien Barré, José A Carrillo, Pierre Degond, Diane Peurichard, and Ewelina Zatorska. Particle interactions mediated by dynamical networks: assessment of macroscopic descriptions. *Journal of nonlinear science*, 28:235–268, 2018.
- [7] Julien Barré, Pierre Degond, and Ewelina Zatorska. Kinetic theory of particle interactions mediated by dynamical networks. *Multiscale Modeling & Simulation*, 15(3):1294–1323, 2017.
- [8] Julien Barré, Paul Dobson, Michela Ottobre, and Ewelina Zatorska. Fast non-mean-field networks: Uniform in time averaging. *SIAM Journal on Mathematical Analysis*, 53(1):937–972, 2021.
- [9] Fabian Baumann, Philipp Lorenz-Spreen, Igor M Sokolov, and Michele Starnini. Modeling echo chambers and polarization dynamics in social networks. *Physical Review Letters*, 124(4):048301, 2020.
- [10] Roger L. Berger. A necessary and sufficient condition for reaching a consensus using DeGroot’s method. *Journal of the American Statistical Association*, 76(374):415–418, 1981.
- [11] Rico Berner, Thilo Gross, Christian Kuehn, Jürgen Kurths, and Serhiy Yanchuk. Adaptive dynamical networks. *Physics Reports*, 1031:1–59, 2023. Adaptive dynamical networks.
- [12] Mathieu Besançon, Theodore Papamarkou, David Anthoff, Alex Arslan, Simon Byrne, Dahua Lin, and John Pearson. Distributions.jl: Definition and Modeling of Probability Distributions in the JuliaStats Ecosystem. *Journal of Statistical Software*, 98(16):1–30, 2021.
- [13] Laurent Boudin and Francesco Salvarani. A kinetic approach to the study of opinion formation. *ESAIM: Mathematical Modelling and Numerical Analysis*, 43(3):507–522, 2 2009.
- [14] Giulia Braghini and Francesco Salvarani. Effects of hidden opinion manipulation in microblogging platforms. *Advances in Complex Systems*, 24(05):2150009, 2021. 10.1142/S0219525921500090.
- [15] Heather Z. Brooks and Mason A. Porter. A model for the influence of media on the ideology of content in online social networks. *Physical Review Research*, 2(2):023041, 2020.
- [16] Martin Burger. Network structured kinetic models of social interactions. *Vietnam Journal of Mathematics*, 49:937–956, 2021.
- [17] Martin Burger. Kinetic equations for processes on co-evolving networks. *Kinetic and Related Models*, 15(2):187–212, 2022.
- [18] René Carmona. *Lectures on BSDEs, stochastic control, and stochastic differential games with financial applications*. SIAM, 2016.

- [19] Louis-Pierre Chaintron and Antoine Diez. Propagation of chaos: a review of models, methods and applications. ii. applications. *arXiv preprint arXiv:2106.14812*, 2021.
- [20] Louis-Pierre Chaintron and Antoine Diez. Propagation of chaos: a review of models, methods and applications. i. models and methods. *arXiv preprint arXiv:2203.00446*, 2022.
- [21] Yen-Chi Chen. A tutorial on kernel density estimation and recent advances. *Biostatistics & Epidemiology*, 1(1):161–187, jan 2017.
- [22] Jonas Dalege, Mirta Galesic, and Henrik Olsson. Networks of beliefs: An integrative theory of individual- and social-level belief dynamics, Apr 2023.
- [23] Simon Danisch and Julius Krumbiegel. Makie.jl: Flexible high-performance data visualization for Julia. *Journal of Open Source Software*, 6(65):3349, 2021.
- [24] Guillaume Deffuant, David Neau, Frederic Amblard, and Gérard Weisbuch. Mixing beliefs among interacting agents. *Advances in Complex Systems*, 03(01n04):87–98, 2000.
- [25] Pierre Degond, Fanny Delebecque, and Diane Peurichard. Continuum model for linked fibers with alignment interactions. *Mathematical Models and Methods in Applied Sciences*, 26(02):269–318, 2016.
- [26] Pierre Degond, Jian-Guo Liu, Sara Merino-Aceituno, and Thomas Tardiveau. Continuum dynamics of the intention field under weakly cohesive social interaction. *Mathematical Models and Methods in Applied Sciences*, 27(01):159–182, 2017.
- [27] Morris H. Degroot. Reaching a consensus. *Journal of the American Statistical Association*, 69(345):118–121, 1974.
- [28] Reinhard Diestel. *Graph theory*, volume 173 of *Graduate Texts in Mathematics*. Springer-Verlag, Berlin, third edition, 2005.
- [29] G Dimarco, B Perthame, Giuseppe Toscani, and Mattia Zanella. Kinetic models for epidemic dynamics with social heterogeneity. *Journal of Mathematical Biology*, 83(1):4, 2021.
- [30] Zhaogang Ding, Xia Chen, Yucheng Dong, and Francisco Herrera. Consensus reaching in social network DeGroot model: The roles of the self-confidence and node degree. *Information Sciences*, 486:62–72, 2019.
- [31] Yucheng Dong, Zhaogang Ding, Luis Martínez, and Francisco Herrera. Managing consensus based on leadership in opinion dynamics. *Information Sciences*, 397:187–205, 2017.
- [32] Alina Dubovskaya, Susan C. Fennell, Kevin Burke, James P. Gleeson, and Doireann O’Kiely. Analysis of mean-field approximation for Deffuant opinion dynamics on networks, 2022.
- [33] Bertram Düring, Peter Markowich, Jan-Frederik Pietschmann, and Marie-Therese Wolfram. Boltzmann and Fokker–Planck equations modelling opinion formation in the presence of strong leaders. *Proceedings of the Royal Society A: Mathematical, Physical and Engineering Sciences*, 465(2112):3687–3708, 2009.
- [34] Simone Fagioli and Gianluca Favre. Opinion formation on evolving network: the DPA method applied to a nonlocal cross-diffusion PDE-ODE system. *European Journal of Applied Mathematics*, page 1–28, 2024.
- [35] Simone Fagioli and Emanuela Radici. Opinion formation systems via deterministic particles approximation. *Kinetic and Related Models*, 14(1):45–76, 2021.
- [36] James Fairbanks, Mathieu Besançon, Schölly Simon, Júlio Hoffman, Nick Eubank, and Stefan Karpinski. Juliagraphs/graphs.jl: an optimized graphs package for the julia programming language, 2021.
- [37] Andreas Flache, Michael Mäs, Thomas Feliciani, Edmund Chattoe-Brown, Guillaume Deffuant, Sylvie Huet, and Jan Lorenz. Models of social influence: Towards the next frontiers. *J. Artif. Soc. Soc. Simul.*, 20, 2017.
- [38] Dimitris Floros. LFRBenchmarkGraphs.jl, 2024.
- [39] John. R. P. French. A formal theory of social power. *Psychological Review*, 3(63):181–194, 1956.
- [40] N. E. Friedkin and E. C. Johnsen. Social influence network theory: A sociological examination of small group dynamics. *Cambridge University Press*, 2011.
- [41] Noah E. Friedkin and Eugene C. Johnsen. Social influence and opinions. *The Journal of Mathematical Sociology*, 15(3-4):193–206, 1990.

- [42] S. Gershgorin. Über die Abgrenzung der Eigenwerte einer Matrix. *Bull. Acad. Sci. URSS*, 1931(6):749–754, 1931.
- [43] Marios A. Gkogkas, Christian Kuehn, and Chuang Xu. Continuum limits for adaptive network dynamics. *Communications in Mathematical Sciences*, 21(1):83–106, 2023.
- [44] Marios Antonios Gkogkas and Christian Kuehn. Graphop mean-field limits for kuramoto-type models. *SIAM Journal on Applied Dynamical Systems*, 21(1):248–283, 2022.
- [45] Marios Antonios Gkogkas, Christian Kuehn, and Chuang Xu. Mean field limits of co-evolutionary heterogeneous networks, 2023.
- [46] F. Harary. A criterion for unanimity in French’s theory of social power. *Studies in social power*, pages 168–182, 1959.
- [47] Rainer Hegselmann, Ulrich Krause, et al. Opinion dynamics and bounded confidence models, analysis, and simulation. *Journal of artificial societies and social simulation*, 5(3), 2002.
- [48] Pierre-Emmanuel Jabin and Sebastien Motsch. Clustering and asymptotic behavior in opinion formation. *J. Differential Equations*, 257(11):4165–4187, 2014.
- [49] Pierre-Emmanuel Jabin, David Poyato, and Juan Soler. Mean-field limit of non-exchangeable systems. 2021.
- [50] József Sznajd Katarzyna Sznajd-Weron. Opinion evolution in closed community. *Int. Journal of Modern Physics C*, 11(6):1157–1165, 2000.
- [51] Christian Kuehn. Network dynamics on graphops. *New Journal of Physics*, 22(5):053030, may 2020.
- [52] Christian Kuehn and Carlos Pulido. Mean-field limits for stochastic interacting particles on digraph measures, 2024.
- [53] Christian Kuehn and Cinzia Soresina. Cross-diffusion induced instability on networks. *Journal of Complex Networks*, 12(2):cnad052, 02 2024.
- [54] Andrea Lancichinetti, Santo Fortunato, and Filippo Radicchi. Benchmark graphs for testing community detection algorithms. *Physical Review E*, 78(4):046110+, October 2008.
- [55] Joseph LaSalle and Solomon Lefschetz. *Stability by Liapunov’s direct method, with applications*, volume Vol. 4 of *Mathematics in Science and Engineering*. Academic Press, New York-London, 1961.
- [56] Keith Lehrer. Social consensus and rational agnology. *Synthese*, 31(1):141–160, 1975.
- [57] Randall J LeVeque. *Finite volume methods for hyperbolic problems*, volume 31. Cambridge university press, 2002.
- [58] Nadia Loy, Matteo Raviola, and Andrea Tosin. Opinion polarization in social networks. *Philosophical Transactions of the Royal Society A*, 380(2224):20210158, 2022.
- [59] Sebastien Motsch and Eitan Tadmor. Heterophilious dynamics enhances consensus. *SIAM review*, 56(4):577–621, 2014.
- [60] C. Th Nguyen. Echo chambers and epistemic bubbles. *Episteme*, 17(2):141–161, 2020.
- [61] Andrew Nugent, Susana N Gomes, and Marie-Therese Wolfram. On evolving network models and their influence on opinion formation. *Physica D: Nonlinear Phenomena*, 456:133914, 2023.
- [62] Andrew Nugent, Susana N. Gomes, and Marie-Therese Wolfram. Steering opinion dynamics through control of social networks, 2024.
- [63] Marco Nurisso, Matteo Raviola, and Andrea Tosin. Network-based kinetic models: Emergence of a statistical description of the graph topology. *European Journal of Applied Mathematics*, page 1–22, 2024.
- [64] Thierry Paul and Emmanuel Trélat. From microscopic to macroscopic scale equations: mean field, hydrodynamic and graph limits. *arXiv preprint arXiv:2209.08832*, 2022.
- [65] Anton V. Proskurnikov and Roberto Tempo. A tutorial on modeling and analysis of dynamic social networks. Part II. *Annual Reviews in Control*, 45:166–190, 2018.
- [66] Sarita Rosenstock, Justin Bruner, and Cailin O’Connor. In epistemic networks, is less really more? *Philosophy of Science*, 84(2):234–252, 2017.

- [67] Jakub Sawicki, Rico Berner, Sarah A. M. Loos, Mehrnaz Anvari, Rolf Bader, Wolfram Barfuss, Nicola Botta, Nuria Brede, Igor Franović, Daniel J. Gauthier, Sebastian Goldt, Aida Hajizadeh, Philipp Hövel, Omer Karin, Philipp Lorenz-Spreen, Christoph Miehl, Jan Mölter, Simona Olmi, Eckehard Schöll, Alireza Seif, Peter A. Tass, Giovanni Volpe, Serhiy Yanchuk, and Jürgen Kurths. Perspectives on adaptive dynamical systems. *Chaos: An Interdisciplinary Journal of Nonlinear Science*, 33(7):071501, 07 2023.
- [68] S. J. Sheather and M. C. Jones. A reliable data-based bandwidth selection method for kernel density estimation. *Journal of the Royal Statistical Society. Series B (Methodological)*, 53(3):683–690, 1991.
- [69] Frantisek Slanina and Hynek Lavicka. Analytical results for the Sznajd model of opinion formation. *The European Physical Journal B-Condensed Matter and Complex Systems*, 35:279–288, 2003.
- [70] Beth M Stokes, Samuel E Jackson, Philip Garnett, and Jingxi Luo. Extremism, segregation and oscillatory states emerge through collective opinion dynamics in a novel agent-based model. *The Journal of Mathematical Sociology*, 48(1):42–80, 2024.
- [71] Alain-Sol Sznitman. Topics in propagation of chaos. *Ecole d’été de probabilités de Saint-Flour XIX—1989*, 1464:165–251, 1991.
- [72] Ye Tian, Peng Jia, Anahita Mirtabatabaei, Long Wang, Noah E Friedkin, and Francesco Bullo. Social power evolution in influence networks with stubborn individuals. *IEEE Transactions on Automatic Control*, 67(2):574–588, 2021.
- [73] Cody Turner. Online echo chambers, online epistemic bubbles, and open-mindedness. *Episteme*, page 1–26, 2023.
- [74] K. JS. Zollman. Social network structure and the achievement of consensus. *Politics, Philosophy & Economics*, 1(1):26–44, 2012.

FACULTY OF MATHEMATICS, UNIVERSITY OF VIENNA, OSKAR-MORGENSTERN-PLATZ 1, 1090, VIENNA, AUSTRIA

Email address: gianluca.favre@univie.ac.at

DEPARTMENT OF MATHEMATICS AND SCIENTIFIC COMPUTING, UNIVERSITY OF GRAZ, HEINRICH-STRASSE 36, 8010, GRAZ (AUSTRIA).

Email address: gaspard.jankowiak@uni-graz.at

FACULTY OF MATHEMATICS, UNIVERSITY OF VIENNA, OSKAR-MORGENSTERN-PLATZ 1, 1090, VIENNA (AUSTRIA).

COMPLEXITY SCIENCE HUB (EXTERNAL FACULTY MEMBER), JOSEFSTÄDTER STRASSE 39, 1080, VIENNA (AUSTRIA).

Email address: sara.merino@univie.ac.at

DEPARTMENT OF MATHEMATICS AND SCIENTIFIC COMPUTING, UNIVERSITY OF GRAZ, HEINRICH-STRASSE 36, 8010, GRAZ (AUSTRIA).

Email address: lara.trussardi@uni-graz.at